AD-A117 989 ARMY ENGINEER WATERWAYS EXPERIMENT STATION VICKSBURG--ETC F/G 12/1
THEORY AND CALCULATION OF THE NONLINEAR ENERGY TRANSFER BETWEEN--ETC(U)
MAY 82 B A TRACY, D T RESIO

UNCLASSIFIED WIS-11 NL

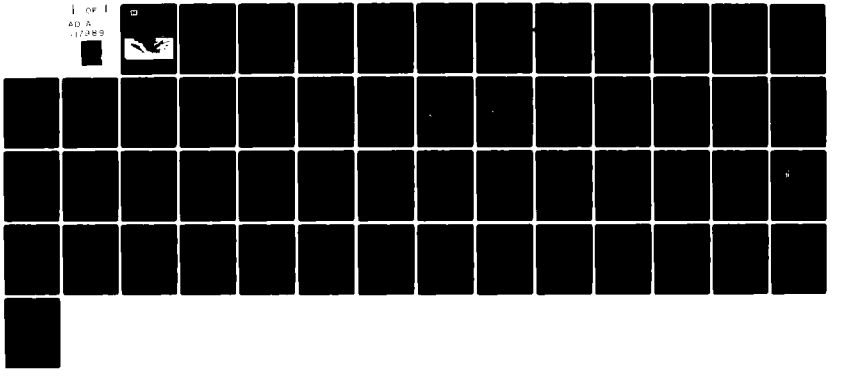

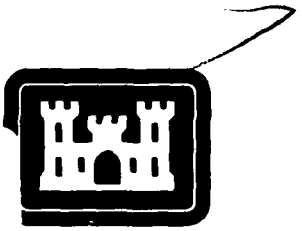

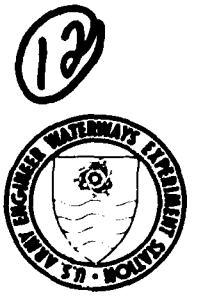

12

THEORY AND CALCULATION OF THE NONLINEAR ENERGY TRANSFER BETWEEN SEA WAVES IN DEEP WATER

by

Barbara A. Tracy, Donald T. Resio

Hydraulics Laboratory
U. S. Army Engineer Waterways Experiment Station
P. O. Box 631, Vicksburg, Miss. 39180

WIS Report 11
May 1982

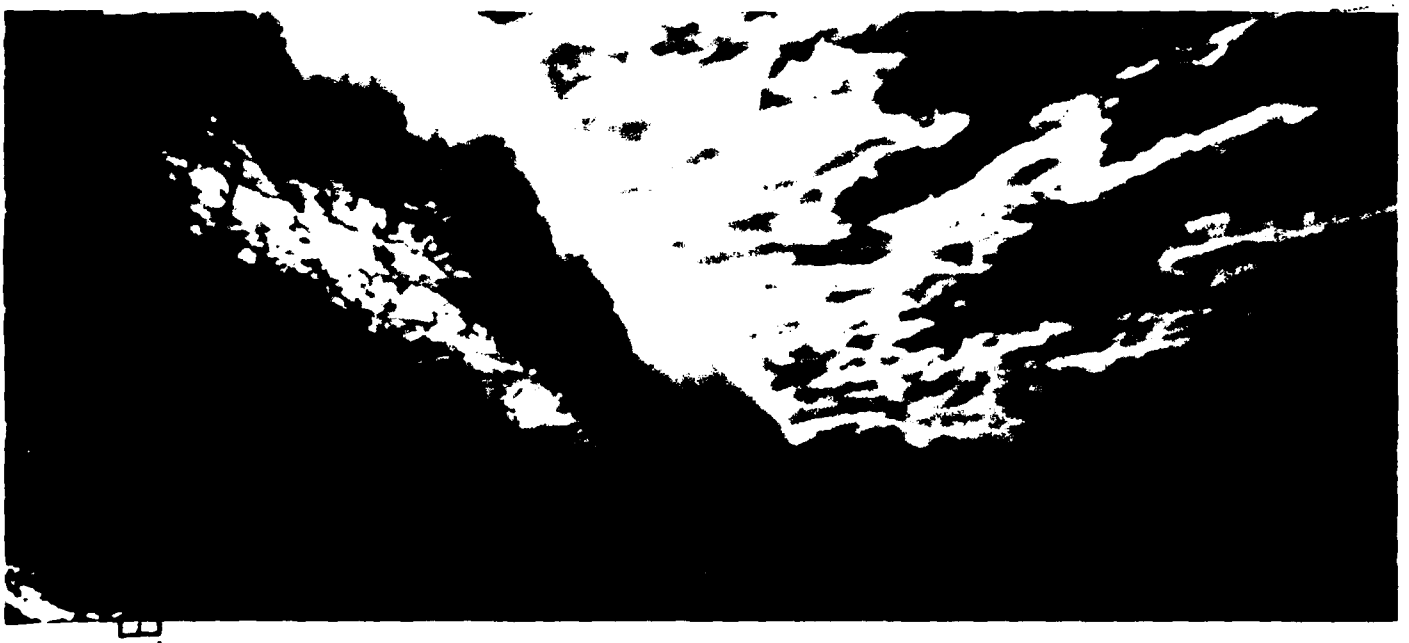

WAVE INFORMATION STUDIES OF U.S. COASTLINES

Prepared for Office, Chief of Engineers, U.S. Army
Washington, D.C. 20314

Destroy this report when no longer needed. Do not return it to the originator.

The findings in this report are not to be construed as an official Department of the Army position unless so designated by other authorized documents.

The contents of this report are not to be used for advertising, publication, or promotional purposes. Citation of trade names does not constitute an official endorsement or approval of the use of such commercial products.

Cover photo by Steve Lissau. Photo originally appeared in *Oceans*, a publication of the Oceanic Society, Vol. 12, No. 1, Jan-Feb 1979.

Unclassified

SECURITY CLASSIFICATION OF THIS PAGE (When Data Entered)

REPORT DOCUMENTATION PAGE	READ INSTRUCTIONS BEFORE COMPLETING FORM
1. REPORT NUMBER: WIS Report 11	2. GOVT ACCESSION NO.: AD-A117 887
	3. RECIPIENT'S CATALOG NUMBER
4. TITLE (and Subtitle): THEORY AND CALCULATION OF THE NONLINEAR ENERGY TRANSFER BETWEEN SEA WAVES IN DEEP WATER	5. TYPE OF REPORT & PERIOD COVERED: Final report
	6. PERFORMING ORG. REPORT NUMBER
7. AUTHOR(s): Barbara A. Tracy Donald T. Resio	8. CONTRACT OR GRANT NUMBER(s)
9. PERFORMING ORGANIZATION NAME AND ADDRESS: U. S. Army Engineer Waterways Experiment Station Hydraulics Laboratory P. O. Box 631, Vicksburg, Miss. 39180	10. PROGRAM ELEMENT, PROJECT, TASK AREA & WORK UNIT NUMBERS
11. CONTROLLING OFFICE NAME AND ADDRESS: Office, Chief of Engineers U. S. Army Washington, D. C. 20314	12. REPORT DATE: May 1982
	13. NUMBER OF PAGES: 47
14. MONITORING AGENCY NAME & ADDRESS (if different from Controlling Office)	15. SECURITY CLASS. (of this report): Unclassified
	15a. DECLASSIFICATION/DOWNGRADING SCHEDULE

16. DISTRIBUTION STATEMENT (of this Report)

Approved for public release; distribution unlimited.

17. DISTRIBUTION STATEMENT (of the abstract entered in Block 20, if different from Report)

18. SUPPLEMENTARY NOTES

Available from National Technical Information Service, 5285 Port Royal Road, Springfield, Va. 22151.

19. KEY WORDS (Continue on reverse side if necessary and identify by block number)

Energy transfer
Integral equations, Nonlinear
Ocean waves
Transport theory
Water waves

20. ABSTRACT (Continue on reverse side if necessary and identify by block number)

A procedure to integrate the energy transfer Boltzmann integrals has been set up by Webb using Hasselmann's theoretical development for the nonlinear wave-wave interactions between sea waves. This report discusses how the integration process has been made simpler and more efficient by the utilization of a geometrically spaced polar grid over the spectral region. This grid allows the loci and the coefficients inside the integrand to scale by various multiples of the geometric scaling factor. Numerical results for the nonlinear energy transfer are given for various spectra.

DD FORM 1 JAN 73 1473 EDITION OF 1 NOV 65 IS OBSOLETE

Unclassified

SECURITY CLASSIFICATION OF THIS PAGE (When Data Entered)

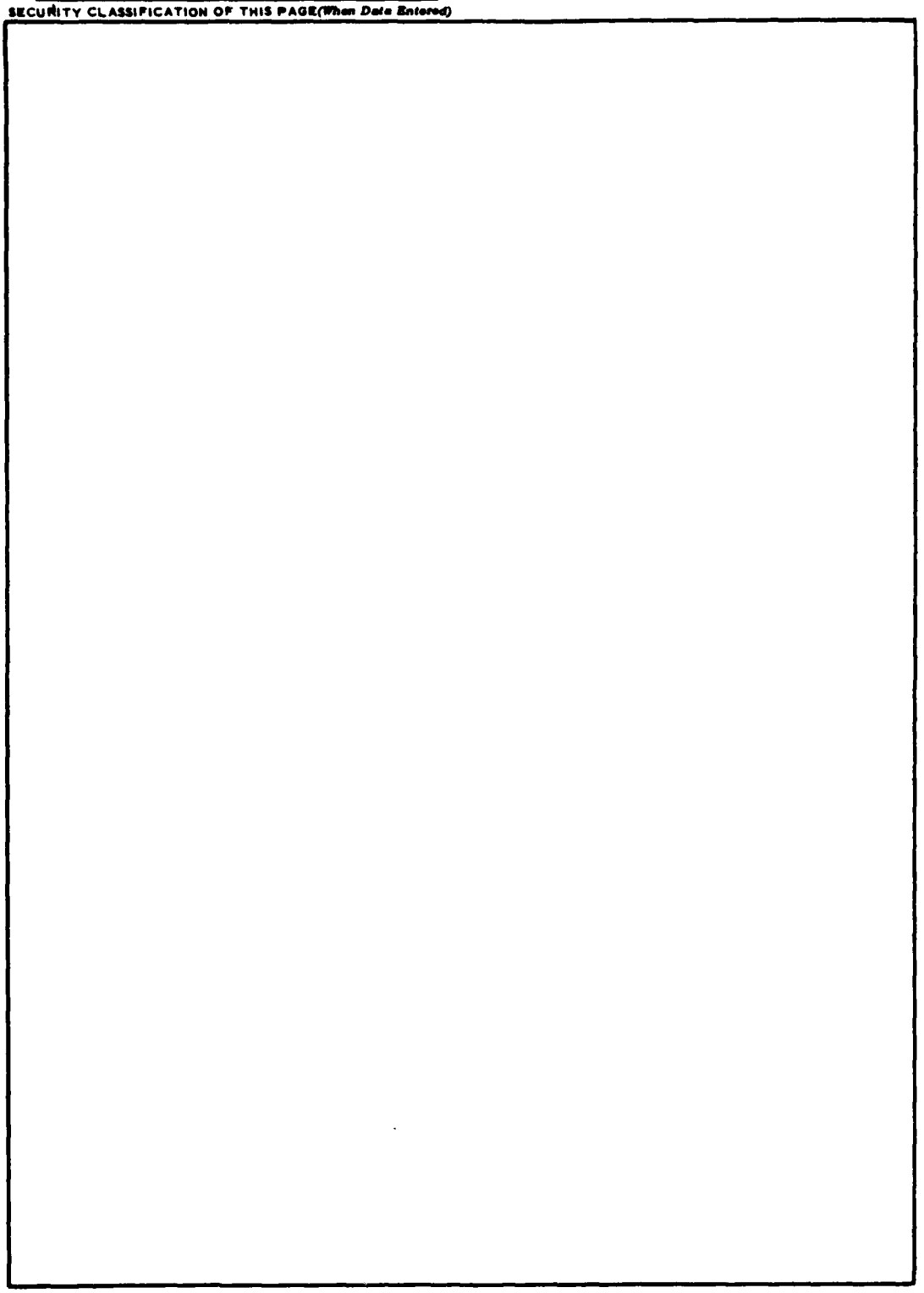

Preface

In late 1976, a study to produce a wave climate for U. S. coastal waters was initiated at the U. S. Army Engineer Waterways Experiment Station (WES). This Wave Information Study (WIS) was authorized by the Office, Chief of Engineers, U. S. Army, as a part of the Field Data Collection Program which is managed by the U. S. Army Coastal Engineering Research Center. The U. S. Army Engineer Division, South Atlantic, and the U. S. Army Engineer Division, New England, also authorized funds during the initial year of this study (FY 1978) to expedite execution of the Atlantic coast portion of this program.

This report, the eleventh in a series, is a technical report describing an integration routine to calculate nonlinear energy transfer for waves in deep water. This work was done in the Hydraulics Laboratory under the direction of Mr. H. B. Simmons, Chief of the Hydraulics Laboratory, Dr. R. W. Whalin, Chief of the Wave Dynamics Division, and Mr. C. E. Chatham, Jr., Chief of the Wave Processes Branch. This report was prepared by Mrs. B. A. Tracy and Dr. D. T. Resio. Mrs. D. S. Ragsdale provided computer assistance, and Miss C. Lanford prepared some of the graphs.

Commanders and Directors of WES during the conduct of the study and the preparation and publication of this report were COL John L. Cannon, CE, COL Nelson P. Conover, CE, and COL Tilford C. Creel, CE. Technical Director was Mr. F. R. Brown.

Contents

THEORY AND CALCULATION OF THE NONLINEAR ENERGY TRANSFER BETWEEN SEA WAVES IN DEEP WATER

Introduction

1. The sea-wave spectrum usually has its main peak just before a low wave-number cutoff. The JONSWAP (Sell and Hasselmann 1972) experiments have shown that this peak is higher and narrower than had been expected, and the peak moves to a lower wave-number cutoff as time increases. Nonlinear interactions between sea waves contribute an energy transfer that could be an explanation for the peak enhancement and the shift to a lower wave-number cutoff. Integral values for the nonlinear energy transfer for a given spectrum can be used to show how this spectral situation changes over a period of time.

2. Nonlinear wave-wave interactions become especially important in the case of tropical wind systems, and the parameterization of wave-wave interaction among components of an asymmetric spectrum is important for the case of tropical systems with rapidly varying wind fields. Experimental data (Forristall et al. 1978) show that the spreading function is frequency-dependent; therefore, different frequency components can propagate in significantly different directions. Investigators feel that the nonlinear transfer may be the reason for extremely long low-energy waves observed after severe storms (Hasselmann 1962). An integration technique that is valid for the nonlinear interactions in a symmetric spectrum can be easily extended to an asymmetric spectral system if that system has an analytical representation.

3. Hasselmann (1962) wrote the equations and evaluated the boundary conditions that model the behavior of a system of waves undergoing nonlinear interactions. These equations involve the rate of change of mean energy (or mean action density) at each wave number. (This energy flux was evaluated by using a perturbation method.) Hasselmann formulated these equations by considering the waves as particles and by considering the whole process as particle scattering. Webb (1978)

has developed an integration approach that evaluates this rate of change of the action density by evaluating the resulting Boltzmann integrals. Development of a special type of grid for this integration scheme allows a fast calculation of the nonlinear energy transfer for a whole spectrum. This grid modification consists of a polar grid with equal angle rays and with radial rings spaced by a geometric progression. A comparison of the results of this method to Webb's results for a Pierson-Moskowitz spectrum is shown. Results for various other symmetric spectral situations are also shown.

Theoretical Development

4. Webb (1978) has taken Hasselmann's equations and written the mean action density equations in terms of a transfer function which gives the rate one wave is scattered into another. The action density form of Hasselmann's equation is*

$$\frac{dn_1}{dt} = \iiint d\vec{k}_1\, d\vec{k}_2\, d\vec{k}_3\, C(\vec{k}_1, \vec{k}_2, \vec{k}_3, \vec{k}_4) \cdot \delta(\vec{k}_1 + \vec{k}_2 - \vec{k}_3 - \vec{k}_4)$$

$$\cdot \delta(\omega_1 + \omega_2 - \omega_3 - \omega_4) \cdot [n_1 n_3 (n_4 - n_2) + n_2 n_4 (n_3 - n_1)] \qquad (1)$$

In this equation, n_i is the action density at wave number $\vec{k}_i$, and ω_i is the angular velocity at $\vec{k}_i$. $\delta(...)$ is the Dirac delta function and $C(...)$ is the coupling coefficient. Energy conservation is taken into account by the angular velocity delta function, and momentum is conserved by the wave-number delta function. The process involves a set of four waves with wave numbers: k_1, k_2, k_3, and k_4. Webb introduces a transfer function $T(\vec{k}_1, \vec{k}_3)$ where

---

* For convenience, symbols and unusual abbreviations are listed and defined in the Notation (Apppendix B).

$$\frac{dn_1}{dt} = \int d\vec{k}_3 \; T(\vec{k}_1,\vec{k}_3) \text{ and}$$

$$T(\vec{k}_1,\vec{k}_3) = 2 \iint d\vec{k}_2 \; d\vec{k}_4 \; C(\vec{k}_1,\vec{k}_2,\vec{k}_3,\vec{k}_4) \; \delta(\vec{k}_1 + \vec{k}_2 - \vec{k}_3 - \vec{k}_4)$$

$$\delta(\omega_1 + \omega_2 - \omega_3 - \omega_4) \cdot \theta\left(|\vec{k}_1 - \vec{k}_4| - |\vec{k}_1 - \vec{k}_3|\right)$$

$$[n_1 n_3 (n_4 - n_2) + n_2 n_4 (n_3 - n_1)] \qquad (2)$$

$$\theta(x) = 1 \text{ if } x > 0$$

$$\theta(x) = 0 \text{ if } x < 0$$

$$x = |\vec{k}_1 - \vec{k}_4| - |\vec{k}_1 - \vec{k}_3| \qquad (3)$$

The $\theta(x)$ function determines a section of the integral which is not defined due to the assumption that $\vec{k}_1$ is closer to $\vec{k}_3$ than $\vec{k}_2$.

5. The transfer function allows us to think of the process as particle scattering where we consider the four waves as four particles with their momentum related to their wave number. The transfer function gives the rate at which $\vec{k}_3$ is scattered into wave $\vec{k}_1$. The density products can be thought of as a diffusing and a pumping density term where $n_1 n_3 (n_4 - n_2)$ is the pumping term and $n_2 n_4 (n_3 - n_1)$ is the diffusive term. The transfer integral can be thought of as a sum of a diffusing transfer integral and a pumping transfer integral.

6. The first consideration in the evaluation of the diffusing and pumping transfer integrals is the limiting properties of the energy and momentum delta functions. We will use the following property of the Dirac delta function (Jackson 1962):

$$\delta(x - a) = 0 \text{ if } x \neq a$$

where x and a are representative functions. $\int \delta(x - a)dx = 1$ if region includes $x = a$, and is zero otherwise. Consider

the $d\vec{k}_4$ part of the transfer integral:

$$\int d\vec{k}_4 \; \delta(\vec{k}_1 + \vec{k}_2 - \vec{k}_3 - \vec{k}_4)$$

If $\vec{k}_1 + \vec{k}_2 - \vec{k}_3 = \vec{k}_4$ for conservation of momentum, the $d\vec{k}_4$ integral equals one and the transfer integral becomes

$$T(\vec{k}_1,\vec{k}_3) = 2\int d\vec{k}_2 \delta(\omega_1 + \omega_2 - \omega_3 - \omega_4) \; F(\vec{k}_1, \ldots) \tag{4}$$

where

$$F(\vec{k}_1, \ldots) = C(\vec{k}_1, \ldots)\theta(x)[n_1 n_3(n_4 - n_2) + n_2 n_4(n_3 - n_1)]$$

This delta function evaluation limits the wave number configuration to $\vec{k}_1 + \vec{k}_2 - \vec{k}_3 = \vec{k}_4$ or $\vec{k}_1 - \vec{k}_3 = \vec{k}_4 - \vec{k}_2$. This means that the tips of the four wave-number vectors must form a parallelogram in wave-number space. See Figure 1 for a description of what a wave-number configuration would look like.

7. In order to evaluate the integral numerically, we must fix values for $\vec{k}_1(x,y)$ and $\vec{k}_3(x,y)$ and consider the limiting properties of the angular velocity delta function. Then, for each set of $(\vec{k}_1,\vec{k}_3)$, let $W(\vec{k}_2)$ equal the argument of the angular velocity delta function. To eliminate the angular velocity delta function, let $W(\vec{k}_2)$ be equal to zero; then

$$W(\vec{k}_2) = 0 = \omega_1 + \omega(\vec{k}_2) - \omega_3 - \omega_4 \; (\vec{k}_1 + \vec{k}_2 - \vec{k}_3) \tag{5}$$

The momentum conservation condition has been used to rewrite $\vec{k}_4$. Consider a $\vec{k}_1$, $\vec{k}_2$, $\vec{k}_3$ coordinate system--one point in the $\vec{k}_1 - \vec{k}_3$ plane would have a whole line of solutions parallel to the $\vec{k}_2$-axis. The set of solutions that will satisfy the conservation conditions can be represented as an egg-shaped two-dimensional locus in a Cartesian coordinate system in $\vec{k}_2$ space where k_{2x} is the x-axis and k_{2y} is the y-axis. On this locus $\vec{n}$ is in the normal or radial direction and $\vec{s}$

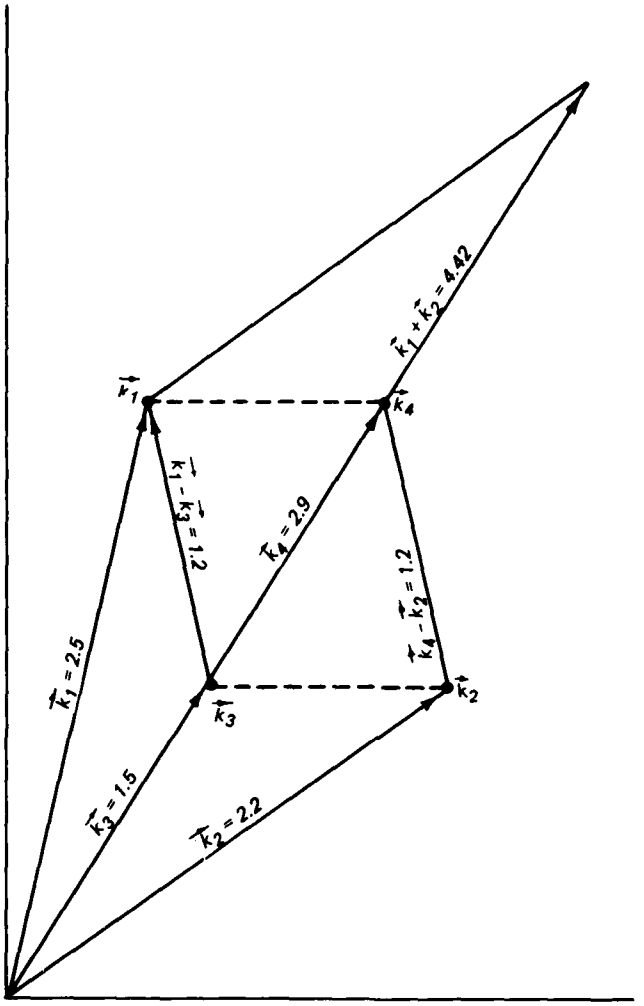

Figure 1. A set of four wave numbers, $\vec{k}_1$, $\vec{k}_2$, $\vec{k}_3$, and $\vec{k}_4$, where $\vec{k}_1 + \vec{k}_2 - \vec{k}_3 = \vec{k}_4$ $\left(|\vec{k}_1|$ is written as $k_1\right)$

is in the increasing θ or tangential direction (see Figure 2).

8. Using a $(\vec{n}, \vec{s})$ coordinate system for $W(\vec{k}_2)$, the transfer integral can be written in terms of the new coordinate system:

$$T(\vec{k}_1,\vec{k}_3) = 2\iint ds\, dn\, \delta[W(\vec{s}, \vec{n})]F(k_1, \ldots) \qquad (6)$$

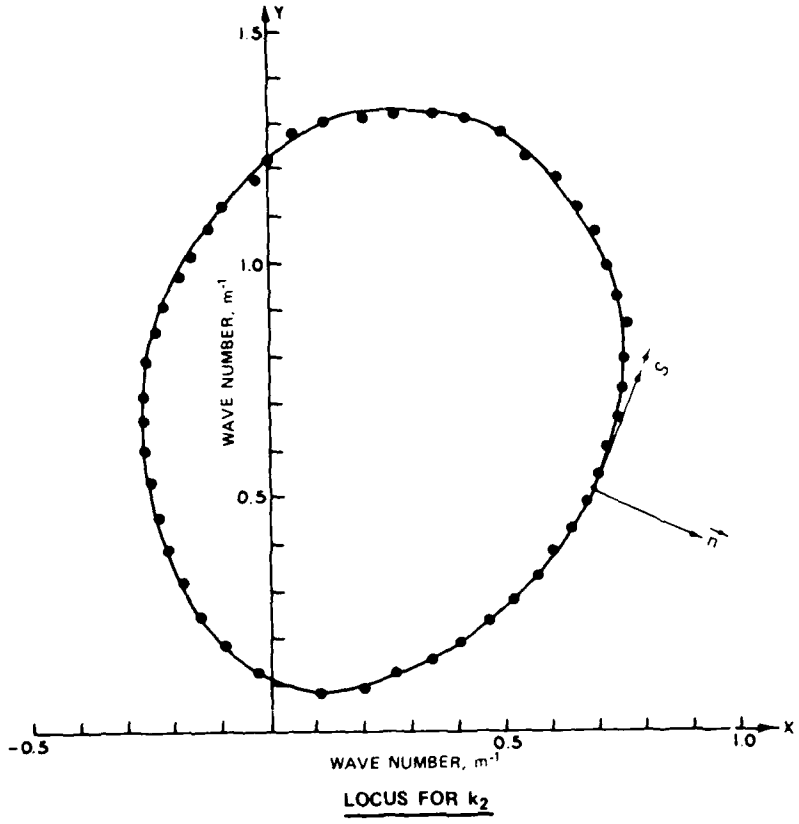

Figure 2. A $(\vec{n},\vec{s})$ coordinate system is set up using the normal and tangential vectors relative to the locus

Another property of the Dirac delta function is (Jackson 1962):

$$\delta[f(x)] = \frac{\delta\ (x - x_o)}{\left|\frac{df}{dx}\right|} \quad \text{where } f(x_o) = 0$$

$$[\delta(f)df = \delta(x)dx]$$

where x and x_o are representative functions. Using this property on $dn \cdot \delta[W(\vec{s},\vec{n})]$, we find that $\delta[W(\vec{s},\vec{n})] = \frac{\delta\ (n - 0)}{\left|\frac{\partial W(\vec{s},\vec{n})}{\partial n}\right|}$. We must integrate

around the s-curve for this property to hold, so

$$T(\vec{k}_1,\vec{k}_3) = 2\iint ds\, dn\, \frac{\delta(n-0)}{\left|\frac{\partial W(\vec{s},\vec{n})}{\partial n}\right|} \cdot F(k_1, \ldots)$$

$$= 2\oint \frac{ds}{\left|\frac{\partial W(\vec{s},\vec{n})}{\partial n}\right|} F(k_1, \ldots) \qquad (7)$$

since $\int dn\, \delta(n-0) = 1$. (Note that evaluation of the integral now reduces to evaluation of a line integral or contour.) The normal derivative in the denominator is the magnitude of a gradient and can be written:

$$\left|\frac{\partial W(\vec{s},\vec{n})}{\partial n}\right|^{-1} = |\nabla W(k_{2x},k_{2y})|^{-1} \qquad (8)$$

This term can be thought of as a phase space term.

9. The evaluation of the integral now entails evaluation of all the factors of the integrand at a series of evenly spaced points along the k_2-contour loop or locus. The factors of the integrand include the phase space term, the coupling coefficient, and the density function. Each of these will be dealt with separately. Figures 3 and 4 show how these three terms behave over a representative locus. A representative locus is also shown in Figure 5. Fifty evenly spaced increments are shown as the points on the locus.

10. The phase space term $\left|\frac{\partial W}{\partial n}\right|$ can be evaluated at each point of the locus by evaluating the gradient of the locus equation (Equation 5). For deep water $\omega \propto k^{1/2}$ ($k = |\vec{k}|$). The locus equation can be simplified by using $Q = k_1^{1/2} - k_3^{1/2}$ (since k_1 and k_3 will remain constant during calculation of the k_2-contour) and defining a new $\vec{P}$-vector, $\vec{P} = \vec{k}_1 - \vec{k}_3$. Each interaction can be defined by a specific $\vec{P}$-vector. After evaluating the ω-functions and substituting for Q and $\vec{P}$, the expression for $W(\vec{k}_2)$ becomes:

$$Q + k_2^{1/2} - \left(|\vec{P} + \vec{k}_2|\right)^{1/2} = 0 \qquad (9)$$

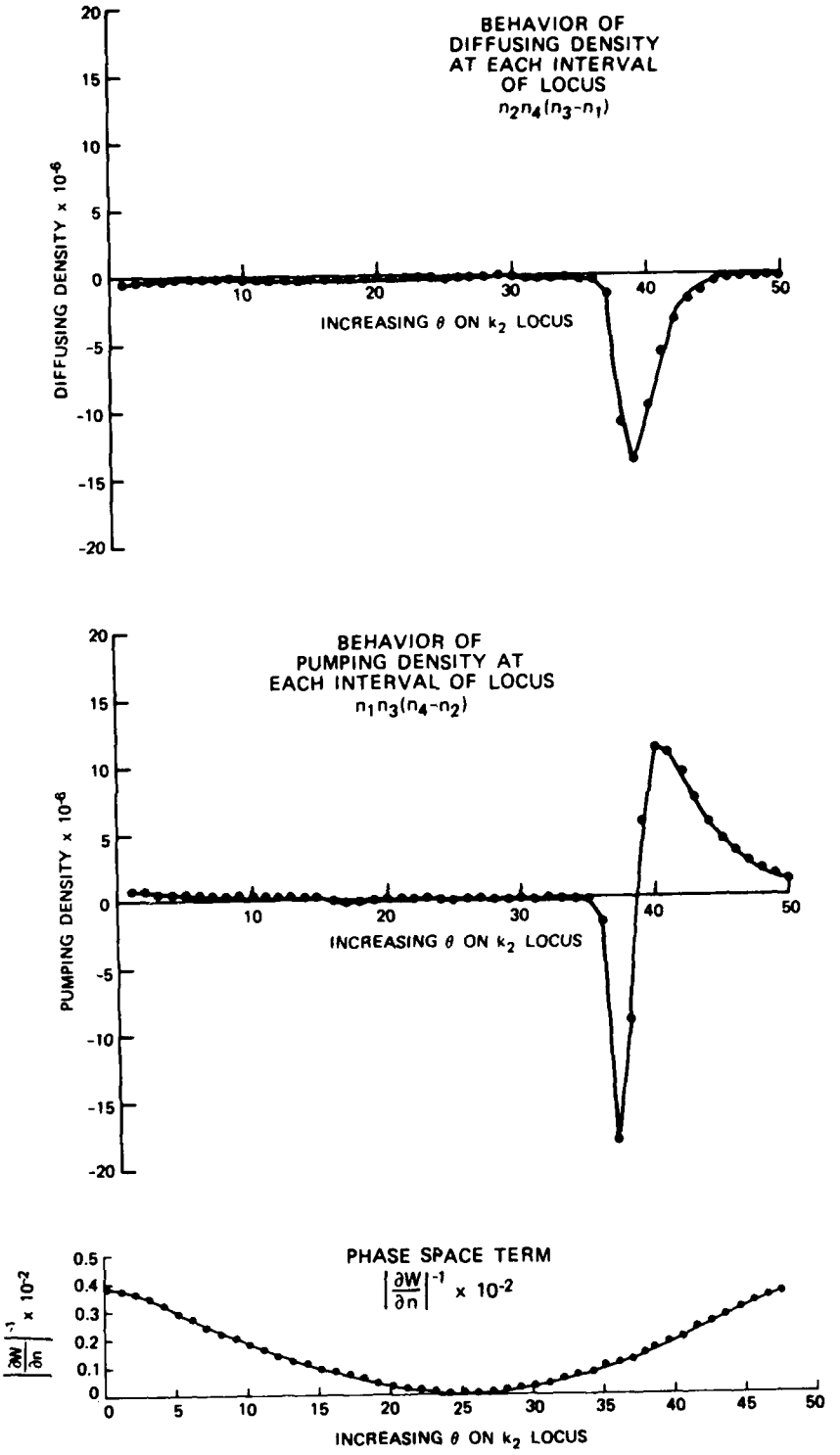

Figure 3. Behavior of the phase space term and density functions over a representative locus

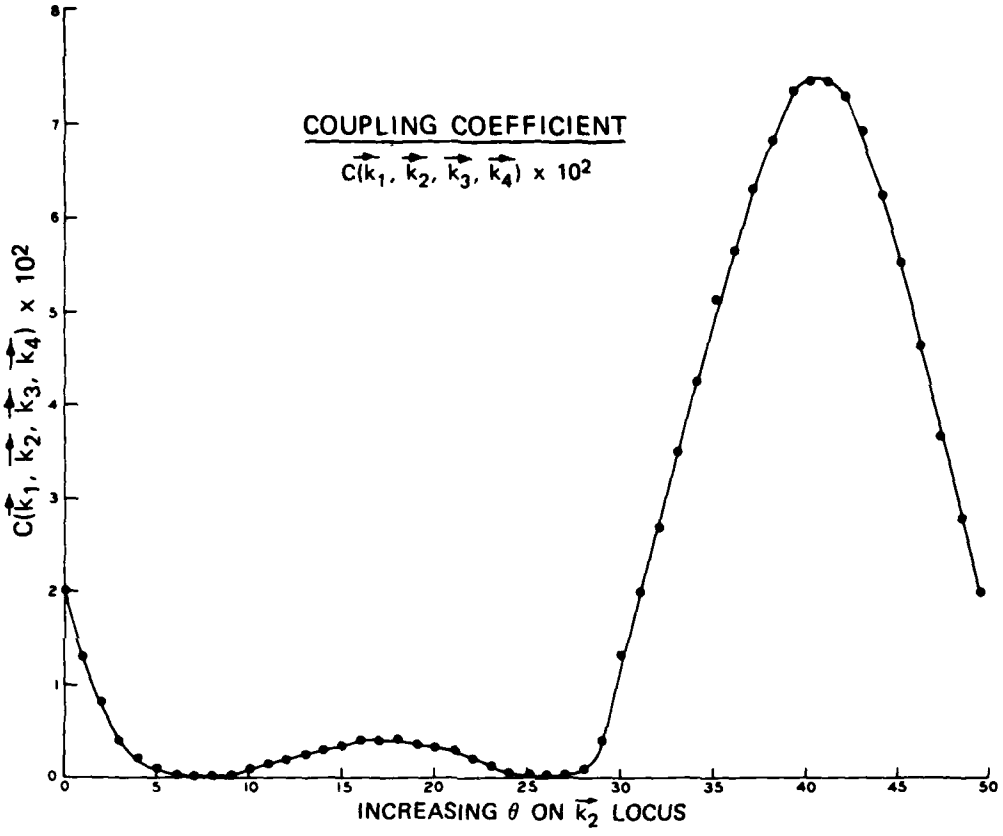

Figure 4. Behavior of the coupling coefficient over a representative locus

The gradient of W is:

$$\nabla W = \frac{\partial W}{\partial x}\,\hat{i} + \frac{\partial W}{\partial y}\,\hat{j} \tag{10}$$

where

$$\frac{\partial W}{\partial x} = \frac{\partial\left[k_2^{1/2} - \left(|\vec{P} + \vec{k}_2|\right)^{1/2}\right]}{\partial x} \tag{11}$$

and

$$\frac{\partial W}{\partial y} = \frac{\partial\left[k_2^{1/2} - \left(|\vec{P} + \vec{k}_2|\right)^{1/2}\right]}{\partial y} \tag{12}$$

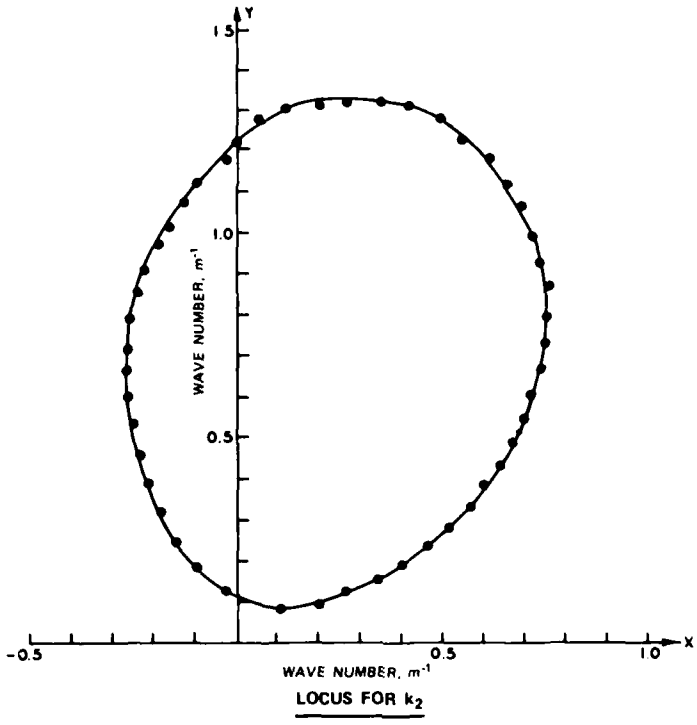

Figure 5. A representative locus in Cartesian coordinates. Locus coordinates have been found by an iteration routine utilizing binary search

Writing the vectors in rectangular components yields:

$$\left(|\vec{P} + \vec{k}_2|\right)^{1/2} = \left[(P_x + x)^2 + (P_y + y)^2\right]^{1/4} \tag{13}$$

where P_x and P_y are the rectangular components of $\vec{P}$ and x and y are the rectangular components of $\vec{k}_2$. The magnitude of the gradient in the normal direction is:

$$|\nabla W| = \left[\left(\frac{\partial W}{\partial x}\right)^2 + \left(\frac{\partial W}{\partial y}\right)^2\right]^{1/2}$$

$$= \left(\left\{\frac{x}{2}\,(x^2 + y^2)^{-3/4} - \frac{(P_x + x)}{2}\left[(P_x + x)^2 + (P_y + y)^2\right]^{-3/4}\right\}^2\right.$$

$$+ \left\{\frac{y}{2}\,(x^2 + y^2)^{-3/4} - \frac{(P_y + y)}{2}\left[(P_x + x)^2\right.\right.$$

$$\left.\left. + (P_y + y)^2\right]^{-3/4}\right\}^2\Bigg)^{1/2} \qquad (14)$$

For ease in working with the angles involved, rectangular coordinates were used for evaluation of this term.

11. The coupling coefficient from Hasselmann's work is a complex algebraic expression and in Webb's paper was put in a usable form by an algebraic manipulator. The expression given in Webb's work was used, and the behavior of this term when plotted over a representative locus exhibits the same shape as Webb's curve. The complete algebraic expression is listed in the appendix.

12. The density term in Hasselmann's equation, $n_1 n_3 (n_4 - n_2) + n_2 n_4 (n_3 - n_1)$, can be thought of as the sum of two types of transfer. A diffusive transfer between k_3 and k_1 is described by $n_2 n_4 (n_3 - n_1)$. This diffusive transfer causes a pumped transfer between k_2 and k_4 in $n_1 n_3 (n_4 - n_2)$. The n_i values are action densities and are related to the amount of energy inherent in a given state, k_i. The action density subscripts correspond to the wave-number subscripts. The whole purpose in constructing an evaluation scheme for the Boltzmann-type integrals is to evaluate the rate of change of the action density at a certain wave number and, therefore, get a value for the energy transfer there. Right now, we are interested in knowing the amount of action density we have available to cause this diffusing and pumping effect in the set of four wave numbers, k_1, k_2, k_3, and k_4.

13. The $n_i\,(\vec{k}_i)$ values are directly calculated from the spectrum

that is being considered. Most spectra can be written as an $E(f)$ function where E is energy in m^2/Hz. The independent variable is frequency, but we are dealing in wave-number space so we must transform the energy density function from a function of frequency to a function of wave number. The one-dimensional frequency function was transformed to a two-dimensional function by using a $\cos^2 \theta$ spreading function. The group velocity c_g can be written as:

$$c_g = \frac{\partial \omega}{\partial k} \tag{15}$$

where ω is angular velocity. The identity relating frequency to wave number in deep water is

$$\omega^2 \alpha\ k \quad \text{or} \quad \omega = \sqrt{gk} \tag{16}$$

Then,

$$c_g = \frac{\omega}{2k} = \frac{\sqrt{gk}}{2k} = \frac{1}{2}\sqrt{\frac{g}{k}} \tag{17}$$

The density function $n_i(\vec{k}_i)$ can be written as:

$$n_i(\vec{k}_i) = \frac{F(\vec{k}_i)}{\omega_i} \tag{18}$$

where $F(\vec{k}_i)$ is the two-dimensional spectrum with respect to wave number and ω_i is the angular frequency. The c_g term acts like a modulation term on the amplitude of the wave function making up the $E(f)$ term to enable a transformation from a frequency-dependent function to a wave-number dependent function. The whole procedure amounts to multiplying $E(f)$ by the square of c_g/ω and adding the spreading function by multiplying the whole expression by $\frac{2}{\pi} \cdot \cos^2 \theta$. If we know the wave number, the action density at a specific wave number can be calculated using the above relationships. A Pierson-Moskowitz spectral density function was used in the initial test case to match with Webb's work, but any spectrum with an analytical wave-number representation could be used in the calculations.

Geometric Spacing Technique for Grid

14. So far, the basic aspects of the factors of the integrand have been dealt with. All these hinge on calculation of the k_2-contour or k_2-locus for each $\vec{k}_1 - \vec{k}_3$ interaction. It is possible to calculate a locus by iteration or a combined interpolation-iteration scheme for each separate $(\vec{k}_1, \vec{k}_3)$ couplet, and this would be the approach to the problem if we used a regularly spaced (k, θ) grid. However, using a geometric progression spacing scheme for the k (radial) values allows us to utilize some geometric vector relationships that will permit the estimation of the k_2- and k_4-loci without having to calculate each as an independent function of a $(\vec{k}_1, \vec{k}_3)$ couplet after one locus has been iterated for each possible orientation of the $(\vec{k}_1, \vec{k}_3)$ couplet. In this method an initial value is chosen for the magnitude of k_o where k_o is the smallest value used for r on the (r, θ) grid. We defined our value for k_o to be $0.14\ m^{-1}$ (MKS wave-number units). k_o must be chosen to be a small wave number in the area where very little interaction takes place. In k-space we are using polar coordinates where $|\vec{k}| = r$ and θ is incremented from 0° to 90° in 9° increments. Our first area of reference will be a circle of radius = k_o. The next reference circle around the origin will have $r = \lambda k_o$, where we have specified $\lambda = 1.2$. The next concentric circle will be $\lambda^2 k_o$ and so on. Figure 6 shows the completed grid with $\lambda = 1.2$ and $k_o = 0.14$.

15. For each interaction we need to define a $\vec{P}$-vector $(\vec{P} = \vec{k}_1 - \vec{k}_3)$. This $\vec{P}$-vector will define the orientation of the interaction on the grid. As stated before, each interaction consists of a constant $\vec{k}_1$-vector and a constant $\vec{k}_3$-vector. $|\vec{k}_3|$ will be assumed to be greater than $|\vec{k}_1|$ for ease in calculation. $\vec{P}$ can be calculated from the $\vec{k}_1$- and $\vec{k}_3$-vectors, and there exists a specific $\vec{P}$-vector for each interaction. Considering Figure 7, it is obvious that on rays of constant θ a set of parallel $\vec{P}$-vectors is produced. These parallel $\vec{P}$-vectors can be related to the locus of the initial $\vec{P}$-vector by the λ scaling factor.

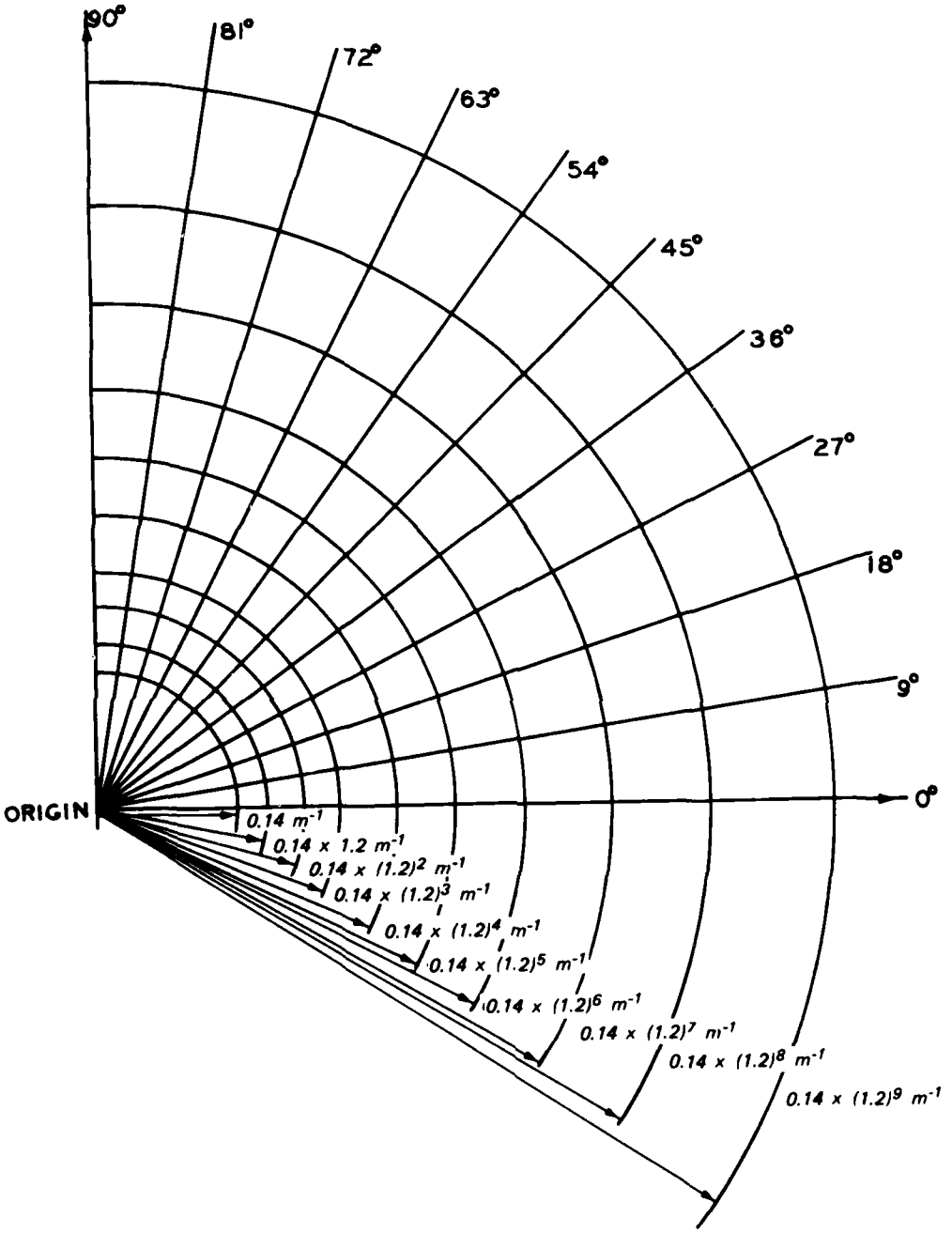

Figure 6. Geometrically spaced polar grid

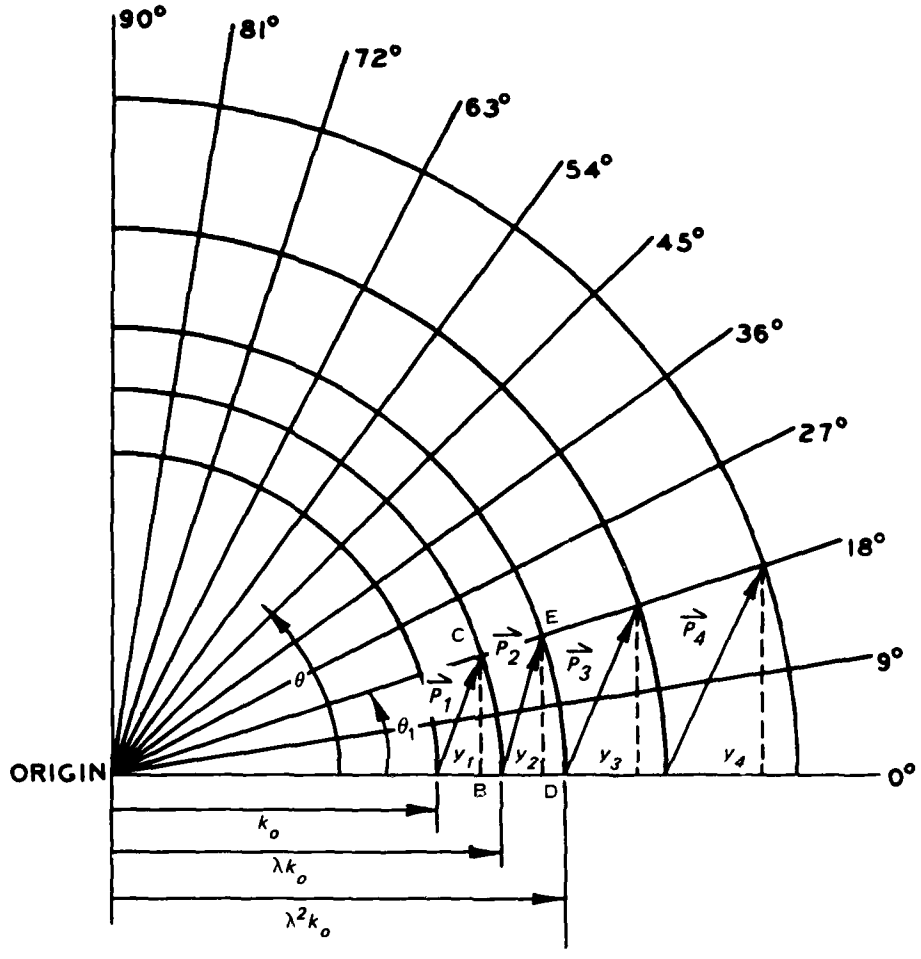

Figure 7. The geometric construction of a set of parallel interaction vectors

16. Considering the geometry in Figure 7 with $\sin \theta_1 = y_1/(\lambda k_o)$ for triangle OBC, the Cartesian coordinates for the orientation of $\vec{P}_1$ (one of the interaction $\vec{P}$-vectors that utilize the $\vec{k}_o$-vector) are:

$$y = \lambda\, k_o \sin \theta_1$$

$$x = \lambda\, k_o \cos \theta_1 - k_o$$

then,

$$|\vec{P}_1| = \sqrt{\lambda^2 k_o^2 \sin^2 \theta_1 + (\lambda k_o \cos \theta_1 - k_o)^2}$$

$$= k_o \sqrt{\lambda^2 + 1 - 2\lambda \cos \theta_1} \qquad (19)$$

The components of $\vec{P}_2$ can be evaluated in the same way using triangle ODE in Figure 7:

$$\sin \theta_1 = \frac{y_2}{\lambda^2 k_o}$$

$$y = \lambda^2 k_o \sin \theta_1$$

$$x = \lambda^2 k_o \cos \theta_1 - \lambda k_o$$

$$|\vec{P}_2| = \sqrt{\left(\lambda^2 k_o \cos \theta_1 - \lambda k_o\right)^2 + \lambda^4 k_o^2 \sin^2 \theta_1}$$

$$= k_o \lambda \sqrt{\lambda^2 + 1 - 2\lambda \cos \theta_1} \qquad (20)$$

Looking at the ratio of $|\vec{P}_2|$ to $|\vec{P}_1|$, we find $|\vec{P}_2| / |\vec{P}_1| = \lambda$. So, the ratio of the magnitude of two consecutive parallel $\vec{P}$-vectors is λ.

17. Considering the locus equation and the relationship between $|\vec{P}_2|$ and $|\vec{P}_1|$, we can show that if we have the locus for the $\vec{P}_1$ interaction, we can calculate the locus for the $\vec{P}_2$ interaction. The locus equation is:

$$Q + k_2^{1/2} - \left(|\vec{P} + \vec{k}_2|\right)^{1/2} = 0 \qquad (21)$$

where

$$Q = k_1^{1/2} - k_3^{1/2} \text{ and } \vec{P} = \vec{k}_1 - \vec{k}_3$$

First, let us write the k_1 and k_3 interaction components (Figure 8) for the locus equation for $\vec{P}_1$:

$$k_3 = \lambda k_o;\ k_{x_3} = \lambda k_o \cos\theta,\ k_{y_3} = \lambda k_o \sin\theta \tag{22}$$

$$k_1 = k_o;\ k_{x_1} = k_o,\ k_{y_1} = 0 \tag{23}$$

Second, the k_1 and k_3 interaction components for the locus for $|\vec{P}_2| = \lambda|\vec{P}_1|$ are:

$$k_1 = \lambda k_o;\ k_{x_1} = \lambda k_o,\ k_{y_1} = 0 \tag{24}$$

$$k_3 = \lambda^2 k_o;\ k_{x_3} = \lambda^2 k_o \cos\theta,\ k_{y_3} = \lambda^2 k_o \sin\theta \tag{25}$$

Substituting the above information we find for the first locus equation:

$$Q = k_o^{1/2} - (\lambda k_o)^{1/2} = k_o^{1/2}(1 - \lambda^{1/2})$$

$$P_{1x} = k_o - \lambda k_o \cos\theta$$

$$P_{1y} = 0 - \lambda k_o \sin\theta$$

$$|\vec{P}_1 + \vec{k}_2| = \sqrt{(P_{1x} + k_{2x})^2 + (P_{1y} + k_{2y})^2}$$

By algebraic manipulations and substitution,

$$|\vec{P}_1 + \vec{k}_2| = \sqrt{k_2^2 + k_{2x}(2k_o)(1 - \lambda\cos\theta) + k_{2y}(2\lambda k_o)(-\sin\theta) + k_o^2(1 + \lambda^2 - 2\lambda\cos\theta)} \tag{26}$$

Using the general locus equation,

$$Q + k_2^{1/2} - \left(|\vec{P} + \vec{k}_2|\right)^{1/2} = 0 \tag{27}$$

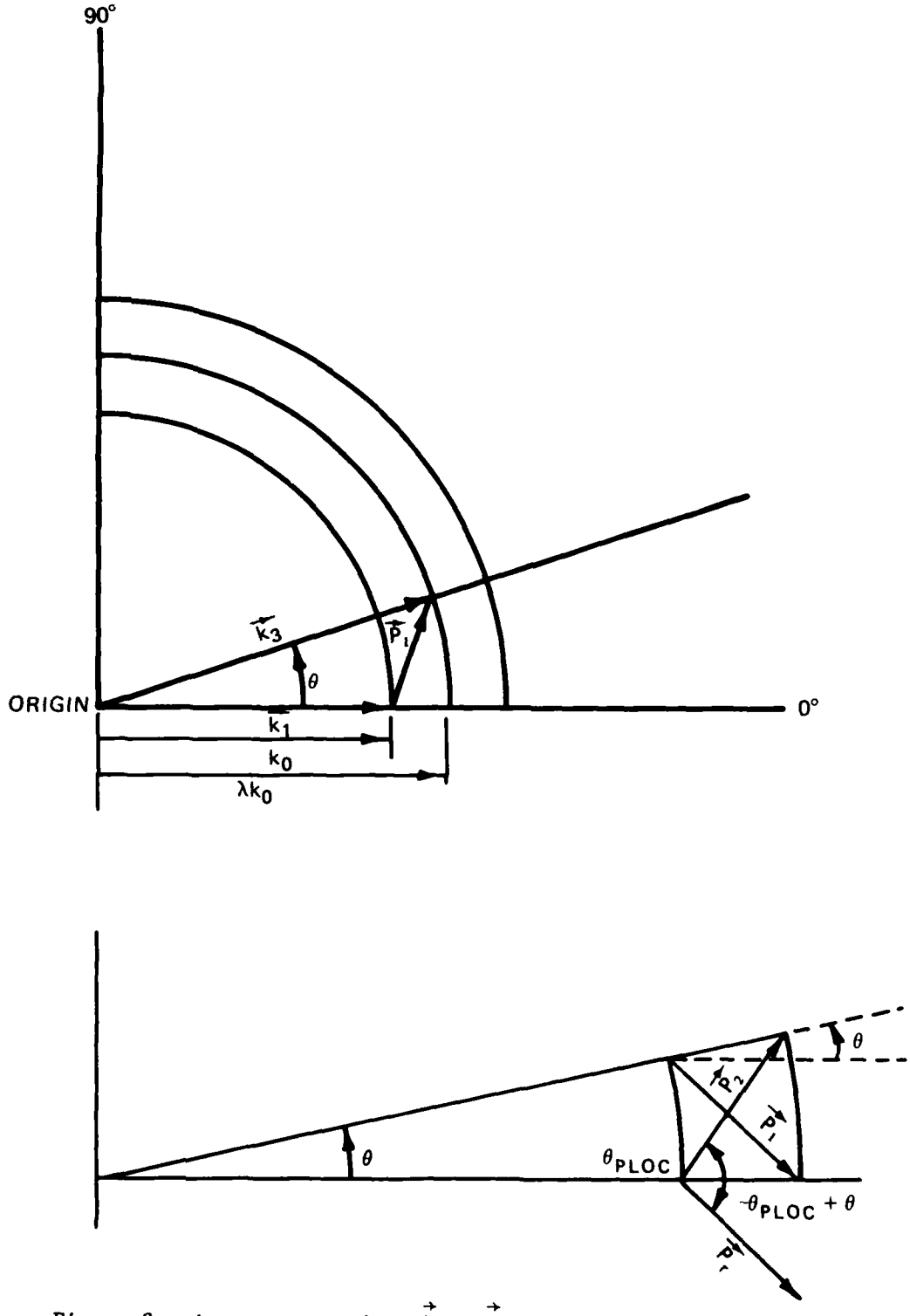

Figure 8. A representative $\vec{k}_3 - \vec{k}_1$ interaction and a geometric construction of a rotated $\vec{P}$-vector

the first locus equation becomes

$$k_o^{1/2}(1 - \lambda^{1/2}) + k_2^{1/2} - \left[k_2^2 + k_{2x}(2k_o)(1 - \lambda \cos\theta) + k_{2y}(2\lambda k_o)(-\sin\theta) + k_o^2(1 + \lambda^2 - 2\lambda \cos\theta)\right]^{1/4} = 0 \qquad (28)$$

Substituting the information for the second locus, we find

$$Q = (\lambda k_o)^{1/2} - \left(\lambda^2 k_o\right)^{1/2} = k_o^{1/2}\lambda^{1/2}(1 - \lambda^{1/2})$$

$$P_{2x} = \lambda k_o - \lambda^2 k_o \cos\theta$$

$$P_{2y} = 0 - \lambda^2 k_o \sin\theta$$

$$|\vec{P}_2 + \vec{k}_2| = \sqrt{(P_{2x} + k_{2x})^2 + (P_{2y} + k_{2y})^2} \qquad (29)$$

By algebraic manipulation and substitution,

$$|\vec{P}_2 + \vec{k}_2| = \sqrt{k_2^2 + k_{2x}(2k_o\lambda)(1 - \lambda\cos\theta) + k_{2y}(-2k_o\lambda^2 \sin\theta) + \lambda^2 k_o^2(\lambda^2 - 2\lambda\cos\theta + 1)} \qquad (30)$$

The second locus equation becomes

$$k_o^{1/2}\lambda^{1/2}(1 - \lambda^{1/2}) + k_2^{1/2} - \left[k_2^2 + k_{2x}(2k_o\lambda)(1 - \lambda\cos\theta) + k_{2y}\left(-2k_o\lambda^2 \sin\theta\right) + \lambda^2 k_o^2(\lambda^2 - 2\lambda\cos\theta + 1)\right]^{1/4} = 0 \qquad (31)$$

18. Using the assumption that the loci scale by a factor of λ, we should be able to substitute $k_{2x_2} = \lambda k_{2x_1}$, $k_{2y_2} = \lambda k_{2y_1}$, and $k_2 = \sqrt{\lambda^2 k_{2x_1}^2 + \lambda^2 k_{2y_1}^2}$ into the second locus and have an algebraic expression equivalent to the expression for the first locus. Substituting, the second locus becomes,

$$k_o^{1/2}\lambda^{1/2}(1 - \lambda^{1/2}) + \left(\lambda^2 k_{2x_1}^2 + \lambda^2 k_{2y_1}^2\right)^{1/4} - \Big[\lambda^2 k_{2x_1}^2 + \lambda^2 k_{2y_1}^2$$

$$+ k_{2x}(2k_o\lambda)(1 - \lambda \cos\theta) + k_{2y}(-2k_o\lambda^2 \sin\theta)$$

$$+ \lambda^2 k_o^2(\lambda^2 - 2\lambda \cos\theta + 1)\Big]^{1/4} = 0 \qquad (32)$$

Divide the above equation by $\lambda^{1/2}$ and it is equivalent to the expression for the first locus equation. Therefore, if we have the coordinates of the initial locus, we can calculate the locus coordinates for any interaction that has a $\vec{P}$-vector parallel to the $\vec{P}$-vector of the initial interaction.

19. In calculation of the loci, we need only calculate a basic set of loci where $k_1 = k_o$, $\theta_1 = 0°$, and k_3 takes the position of each other point of intersection of the grid. Comparisons are shown in Table 1. In this figure we have considered a basic locus where $k_{1x} = 0.1400$, $k_{1y} = 0$, $k_{3x} = 0.2016$, and $k_{3y} = 0$. The x and y coordinates are given for this locus. The next set of values are λ times the coordinates of the basic locus. The third section contains the coordinates for a locus with the same $\vec{P}$-vector coordinates as the second locus. The basic locus and the locus of the third section have been iterated by a binary search routine that will be outlined later in the section on the program method. ($k_{1x} = 0.1680$, $k_{1y} = 0$, $k_{3x} = 0.2419$, and $k_{3y} = 0$ are the interaction components of the second and third loci.) The ratio of the $\vec{P}$-vector of the second locus to the $\vec{P}$-vector of the basic locus is λ. It is obvious that λ times the basic locus coordinates gives locus coordinates that are very close to the iterated locus values. Figures 9 and 10 and Table 2 show two loci where the ratio of P_2 to P_1 is 1.15.

20. The solution to the problem of the calculation of the loci reduces to the calculation of a basic set of loci. The loci for parallel $\vec{P}$-vectors for other higher order interactions can be calculated

Table 1

Comparison of a Basic Locus and a Scaled Locus

Basic Locus for $k_{1x} = 0.1400$, $k_{1y} = 0.0000$, $k_{3x} = 0.2016$, $k_{3y} = 0.0000$		$\lambda = 1.2$ Lambda Times Basic Locus Values		Iterated Locus for $k_{1x} = 0.1680$, $k_{1y} = 0.0000$, $k_{3x} = 0.2419$, $k_{3y} = 0.0000$	
x	y	x	y	x	y
0.2016	0.0	0.2419	0.0	0.2419	0.0
0.2007	0.0098	0.2408	0.0118	0.2409	0.0118
0.1982	0.0193	0.2378	0.0232	0.2378	0.0232
0.1940	0.0282	0.2328	0.0335	0.2329	0.0338
0.1886	0.0362	0.2263	0.0433	0.2264	0.0434
0.1822	0.0432	0.2186	0.0517	0.2187	0.0517
0.1750	0.0489	0.2100	0.0587	0.2100	0.0587
0.1674	0.0537	0.2009	0.0644	0.2008	0.0645
0.1594	0.0575	0.1913	0.0690	0.1913	0.0690
0.1513	0.0603	0.1816	0.0724	0.1815	0.0723
0.1431	0.0622	0.1717	0.0746	0.1717	0.0746
0.1350	0.0633	0.1620	0.0760	0.1620	0.0759
0.1269	0.0636	0.1523	0.0763	0.1523	0.0763
0.1189	0.0633	0.1427	0.0760	0.1427	0.0759
0.1110	0.0623	0.1332	0.0748	0.1332	0.0747
0.1032	0.0606	0.1238	0.0727	0.1239	0.0727
0.0955	0.0583	0.1146	0.0700	0.1146	0.0699
0.0879	0.0523	0.1055	0.0662	0.1054	0.0663
0.0803	0.0515	0.0964	0.0618	0.0964	0.0618
0.0730	0.0469	0.0876	0.0563	0.0876	0.0563
0.0659	0.0415	0.0791	0.0498	0.0790	0.0497
0.0592	0.0340	0.0710	0.0420	0.0710	0.0421
0.0532	0.0276	0.0638	0.0331	0.0638	0.0331
0.0482	0.0192	0.0578	0.0230	0.0579	0.0230
0.0448	0.0099	0.0538	0.0119	0.0538	0.0118
0.0436	0.0000	0.0523	0.0000	0.0524	0.0000
0.0448	-0.0099	0.0538	-0.0119	0.0538	-0.0118
0.0482	-0.0192	0.0578	-0.0230	0.0579	-0.0230
0.0532	-0.0276	0.0638	-0.0331	0.0635	-0.0331
0.0592	-0.0350	0.0710	-0.0420	0.0710	-0.0421
0.0659	-0.0415	0.0791	-0.0498	0.7090	-0.0497
0.0730	-0.0469	0.0876	-0.0562	0.0876	-0.0563
0.0803	-0.0513	0.0964	-0.0618	0.0964	-0.0618
0.0879	-0.0552	0.1055	-0.0662	0.1054	-0.0663
0.0955	-0.0582	0.1146	-0.0698	0.1146	-0.0699
0.1032	-0.0606	0.1238	-0.0727	0.1239	-0.0727
0.1110	-0.0623	0.1332	-0.0748	0.1332	-0.0747
0.1189	-0.0633	0.1427	-0.0760	0.1427	-0.0759
0.1269	-0.0636	0.1523	-0.0763	0.1523	-0.0763
0.1350	-0.0633	0.1620	-0.0760	0.1620	-0.0759
0.1431	-0.0622	0.1717	-0.0746	0.1717	-0.0746
0.1513	-0.0603	0.1816	-0.0724	0.1815	-0.0723
0.1594	-0.0575	0.1913	-0.0690	0.1913	-0.0690
0.1674	-0.0537	0.2009	-0.0644	0.2008	-0.0645
0.1750	-0.0489	0.2100	-0.0587	0.2100	-0.0587
0.1822	-0.0431	0.2186	-0.0517	0.2187	-0.0517
0.1886	-0.0361	0.2263	-0.0433	0.2264	-0.0434
0.1940	-0.0282	0.2325	-0.0338	0.2329	-0.0338
0.1982	-0.0193	0.2378	-0.0232	0.2378	-0.0232
0.2007	-0.0098	0.2408	-0.0118	0.2409	-0.0118

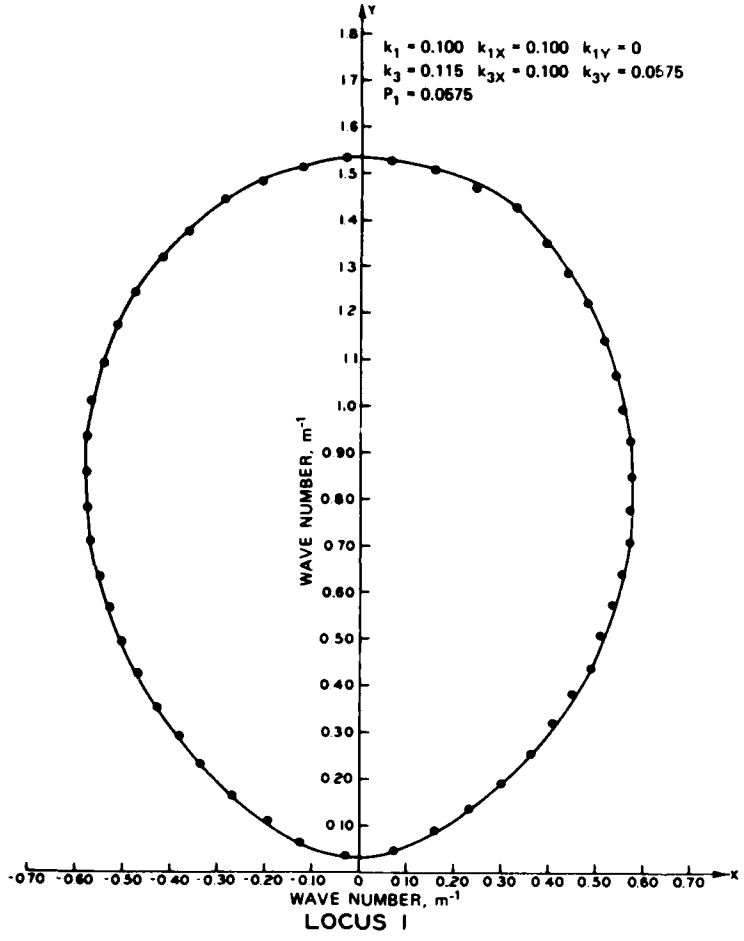

Figure 9. Representative locus (locus 1) used for comparison in Figure 11

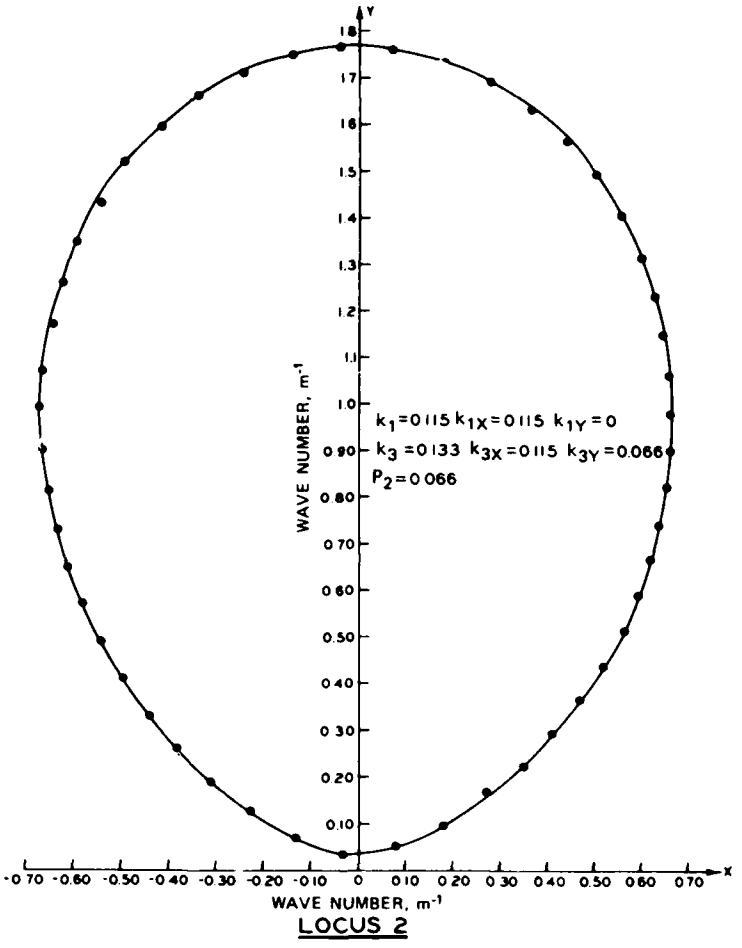

Figure 10. Representative locus (locus 2) used for comparison in Figure 11

Table 2

A Comparison of the Two Loci in Figures 9 and 10

LOCUS 1		LOCUS 2		RATIOS	
k_1=0.100		k_1 = 0.115		$\frac{(k_1)_2}{(k_1)_1}$ = 1.1500	
k_3=0.115		k_3 = 0.133		$\frac{(k_3)_2}{(k_3)_1}$ = 1.1500	
P_1=0.0575		P_2 = 0.066		$\frac{(P)_2}{(P)_1}$ = 1.1478	
x	y	x	y	$\frac{(x)_2}{(x)_1}$	$\frac{(y)_2}{(y)_1}$
0.5756	0.7806	0.6636	0.9000	1.1529	1.1530
0.3891	1.3550	0.4486	1.5623	1.1529	1.1530
-0.1155	1.5151	-0.1334	1.7477	1.1550	1.1535
-0.4703	1.2453	-0.5425	1.4360	1.1535	1.1535
-0.5763	0.8565	-0.6648	0.9875	1.1536	1.1529
-0.5032	0.4904	-0.5805	0.5653	1.1536	1.1527
-0.2664	0.1622	-0.3072	0.1871	1.1532	1.1535
0.1573	0.0852	0.1813	0.0982	1.1526	1.1526
0.4494	0.3817	0.5188	0.4394	1.1544	1.1512
0.5676	0.7120	0.6547	0.8208	1.1535	1.1528

from the basic set. Two other factors of the integrand, $\left|\frac{\partial W}{\partial n}\right|$ and the coupling coefficient, also scale by functions of the λ-scaling factor for the parallel $\vec{P}$-vectors.

21. The phase space term, $\left|\frac{\partial W}{\partial n}\right|^{-1}$, scales by the $\sqrt{\lambda}$. Let $DW_1 = |\partial W/\partial n|^{-1}$ for the basic locus for the interaction listed in Table 1. Let $DW_2 = |\partial W/\partial n|^{-1}$ for the locus that has a $\vec{P}$-vector parallel to the $\vec{P}$-vector which is λ times the first $\vec{P}$-vector as shown in the second column of Table 1. We find that $DW_2/DW_1 = \sqrt{\lambda}$. These ratios are shown in Table 3. The eight values listed here are the calculated $|\partial W/\partial n|^{-1}$ values for the first eight locus coordinates shown in Table 1. Similarly, the coupling coefficient scales by a factor of λ^6. Values of the calculated coupling coefficient for two loci are shown in Table 4 for the same locus coordinates as were used in the above discussion on the phase space term.

22. The $|\partial W/\partial n|^{-1}$ term as stated before is the magnitude of the gradient of the W expression for the locus where $k_2 = \left(k_x^2 + k_y^2\right)^{1/2}$:

$$|\nabla W| = \left[\left(\frac{\partial W}{\partial x}\right)^2 + \left(\frac{\partial W}{\partial y}\right)^2\right]^{1/2}$$

$$= \left(\left\{\frac{k_x}{2}\left(k_x^2 + k_y^2\right)^{-3/4} - \frac{(P_x + k_x)}{2}\left[(P_x + k_x)^2 + (P_y + k_y)^2\right]^{-3/4}\right\}^2 + \left\{\frac{k_y}{2}\left(k_x^2 + k_y^2\right)^{-3/4} - \frac{(P_y + k_y)}{2}\left[(P_x + k_x)^2 + (P_y + k_y)^2\right]^{-3/4}\right\}^2\right)^{1/2} \quad (33)$$

Let $k_x = \lambda k_x$ and $k_y = \lambda k_y$ and $P = \lambda P$. Then

Table 3

Scaling of the Phase Space Term

Phase Space Term $\left\lvert\frac{\partial W}{\partial n}\right\rvert^{-1}_{BL}$	Phase Space Term $\left\lvert\frac{\partial W}{\partial n}\right\rvert^{-1}_{\lambda BL}$	Ratio of Phase Space Terms $\left\lvert\frac{\partial W}{\partial n}\right\rvert^{-1}_{\lambda BL} / \left\lvert\frac{\partial W}{\partial n}\right\rvert^{-1}_{BL}$
Basic Locus $k_1 = (0.14,.00)$ $k_3 = (0.2016,.00)$	λ Times Basic Locus $\lambda = 1.2$ $k_1 = (0.168,.00)$ $k_3 = (0.242,.00)$	$\lambda = 1.2$ $\sqrt{\lambda} = 1.095$
4.49	4.92	1.096
4.44	4.87	1.097
4.31	4.72	1.095
4.11	4.50	1.095
3.85	4.22	1.096
3.58	3.92	1.095
3.29	3.60	1.094
3.00	3.29	1.097

Table 4

Coupling Coefficient

Coupling Coefficient $C_{BL} \times 10^{-3}$	Coupling Coefficient $C_{\lambda BL} \times 10^{-3}$	Ratio of Coupling Coefficients $C_{\lambda BL}/C_{BL}$
Basic Locus $k_1 = (0.14,.00)$ $k_3 = (0.2016,.00)$	λ Times Basic Locus $\lambda = 1.2$ $k_1 = (0.168,.00)$ $k_3 = (0.242,.00)$	$\lambda = 1.2$ $\lambda^6 = 2.986$
0.196	0.586	2.990
.193	.576	2.984
.183	.547	2.989
.168	.502	2.988
.149	.446	2.993
.129	.384	2.976
.108	.323	2.991
.0885	.264	2.983

$$|\nabla W| = \left(\left\{ \frac{\lambda k_x}{2} \left(\lambda^2 k_x^2 + \lambda^2 k_y^2 \right)^{-3/4} - \frac{(P_x + k_x)\lambda}{2} \left[\lambda^2 (P_x + k_x)^2 \right. \right. \right.$$

$$\left. \left. \left. + \lambda^2 (P_y + k_y)^2 \right]^{-3/4} \right\}^2 + \left\{ \frac{\lambda k_y}{2} \left(\lambda^2 k_x^2 + \lambda^2 k_y^2 \right)^{-3/4} \right.$$

$$\left. \left. - \frac{(P_y + k_y)\lambda}{2} \left[\lambda^2 (P_x + k_x)^2 + \lambda^2 (P_y + k_y)^2 \right]^{-3/4} \right\}^2 \right)^{1/2}$$

$$|\nabla W| = \left(\left\{ \lambda^{-1/2} \frac{k_x}{2} \left(k_x^2 + k_y^2 \right)^{-3/4} - \lambda^{-1/2} \frac{(P_x + k_x)}{2} \left[(P_x + k_x)^2 \right. \right. \right.$$

$$\left. \left. \left. + (P_y + k_y)^2 \right]^{-3/4} \right\}^2 + \left\{ \frac{\lambda^{-1/2} k_y}{2} \left(k_x^2 + k_y^2 \right)^{-3/4} \right.$$

$$\left. \left. - \frac{\lambda^{-1/2}(P_y + k_y)}{2} \left[(P_x + k_x)^2 + (P_y + k_y)^2 \right]^{-3/4} \right\}^2 \right)^{1/2}$$

$$= \lambda^{-1/2} \text{ (original } |\nabla W| \text{)} \tag{34}$$

23. All these scaling factors will aid in the numerical evaluation of the transfer integral by allowing us to use one basic set of calculations and the scaling factors to evaluate the interactions for the entire grid. The transfer integral can be written as:

$$T(\vec{k}_1, \vec{k}_3) = \oint F(k_1, \ldots) D(k_1, \ldots) \tag{35}$$

where

$$F\ (k_1,\ \ldots) = \left|\frac{\partial W}{\partial n}\right|^{-1} \cdot C(k_1,\ k_2,\ k_3,\ k_4) \cdot ds$$

Density, $D\ (k_1,\ \ldots)$, is the sum of the diffusing and pumping densities for a given set of four wave numbers and a given spectral representation. Note that the $\theta(x)$ function has been left out of the integral representation since we will not delete a section of the contour as Webb has. The transfer integral can be written as a product of a geometric product term and a density function. The density function is

$$n_1 n_3 (n_4 - n_2) + n_2 n_4 (n_3 - n_1) \tag{36}$$

where n_i is the action density at various wave numbers, k_i. This term can be calculated using the locus coordinates for the specific interaction and the applicable spectral function. The $F\ (k_1,\ \ldots)$ term is a geometric product term depending on the specific locus. When the basic locus coordinates are calculated, a geometric product term is also calculated for each increment of the basic locus. This geometric product factor can be scaled for λ-multiples of the basic loci by a product of the separate scaling terms as defined before. This product of scaling terms is

$$\sqrt{\lambda} \cdot \lambda^6 \cdot \lambda = \lambda^{15/2} \tag{37}$$

The last λ is obtained from the polar differential increment for the integral, $r\ dr\ d\theta$ or ds. The transfer integral can then be written as $T(\vec{k}_1, \vec{k}_3) = \oint D\ (k_1,\ \ldots) \cdot GEOM\ (k_1,\ \ldots) \cdot \lambda^{15/2}$ where the λ value is determined by the interaction being considered. The basic geometric product, $GEOM\ (k_1,\ \ldots)$, is determined by the basic locus that has a $\vec{P}$-vector orientation parallel to the $\vec{P}$-vector of the interaction.

24. The integral in the above form has advantages when using computer evaluation. The product form has a vectorizing potential that will make evaluations of the nonlinear energy transfer for a whole spectrum fast and inexpensive.

25. Going back to the theoretical development, the

nonlinear energy transfer can be written as:

$$\frac{\partial n_1}{\partial t} = \int T(\vec{k}_1, \vec{k}_3)\ d\vec{k}_3 \tag{38}$$

In polar coordinates

$$\frac{\partial n_1}{\partial t} = \int_0^{\infty} \int_0^{2\pi} T(\vec{k}_1, \vec{k}_3)\ d\theta_3 k_3 dk_3 \tag{39}$$

As discussed before, the transfer at a specific orientation of k_1 and k_3 will have an initial value which is a function of the basic locus. This basic value of the transfer integral will be defined as $T_o(\vec{k}_1, \vec{k}_3)$. Each successive transfer integral at the same orientation of $\vec{k}_1$ and $\vec{k}_3$ (parallel $\vec{P}$-vectors) can be written as $\lambda^{15/2} \cdot T_o$.

26. Therefore, at a fixed $k_1 - k_3$ orientation (θ_{13}), the nonlinear energy transfer can be written:

$$\frac{\partial n_1}{\partial t} (\theta_{13} \text{ fixed}) = \int_0^{\infty} (\lambda^{\eta})^{15/2} T_o\ k_3\ d\kappa_3 \tag{40}$$

k_3 can be written as $\lambda^{\eta+1} k_o$ for a specific interaction where η (the number of the radial) begins at zero and progresses to infinity (in reality, the edge of the grid). dk_3 or Δk_3 can be written as $(\lambda^{\eta+1} - \lambda^{\eta}) k_o$. In summation notation, the transfer for one angular section is:

$$\frac{\partial n_1}{\partial t} (\theta_{13} \text{ fixed}) = \sum_{n=0}^{\infty} (\lambda^{\eta})^{15/2} T_o\ \lambda^{\eta+1} k_o (\lambda^{\eta+1} - \lambda^{\eta}) k_o \tag{41}$$

where η is the number of the radial and infinity is the edge of the grid. The total nonlinear transfer for the whole grid can be written as:

$$\frac{\partial n_1}{\partial t} = \sum \frac{\partial n_1}{\partial t} (\theta_{13} \text{ fixed}) \cdot \Delta\theta_{13} \tag{42}$$

where the summation is over all possible θ_{13} orientations.

Program Method

27. A polar geometrically spaced grid as described in the previous section (Figure 6) was set up and used. The numerical results given in this report were obtained by using a grid with $k_o = 0.14$ in MKS wave-number units and $\lambda = 1.1$. The θ increments on the grid were 4.5°. Thirty rings of different r values are used and eleven positive and negative angle increments including zero were used.

28. A set of basic loci was calculated using the above grid parameters. This was done in a separate program, and the output of this program created a tape listing the basic locus coordinates with their corresponding geometric product calculation for each possible interaction angle. To determine the basic loci k_3 assumed the position of each intersection on the grid and k_1 remained equal to k_o and oriented at $\theta = 0°$. All the angular points of each ring were done first, and then the program moved on to the next ring. The loci were stored in this order.

29. To locate the coordinates for each of the basic loci the analytical expression (Equation 9) for the locus equation was solved using $\vec{k}_1$ and $\vec{k}_3$ to find the coordinates $(\vec{k}_2)$ of a point on either end of the egg-shaped locus; then the center for the locus was found by locating the middle point of the line between two points on the ends of the locus. A radius for the locus was calculated from this information and a binary search procedure found 50 evenly spaced points of the locus within an epsilon range of 10^{-6}. The first coordinate of each locus is the point where the $\vec{P}$-vector of the interaction would intersect it. The points continue in a counterclockwise direction until the loop is complete. All the coefficients of the integrand (the coup ing coefficient, the phase term, and the ds term) except the densities are combined into a product and saved for each locus increment. Each of these integrand coefficients was calculated via a subroutine for each point on each locus. These basic locus coordinates and a value for the product (geometric product factor) of the integrand coefficients are available to be read into the main program. The basic loci were read into the main program

and indexed by the difference of the k_3-angle and the k_1-angle, the ring difference between k_3 and k_1, and the number of the increment on the specific locus for the k_1 and k_3 interaction. The geometric products were also indexed by this same scheme. Loops were set up to define the $|\vec{k}|$ values for each point of the grid using the λ-scaling factor and to define the value of the geometric scaling factor $(\lambda^{15/2})$ for each point of the grid. Loops were also set up to determine the values for the angles used in the calculation.

30. The incrementation scheme in the integration program uses a series of four nested do loops. The outermost loop is the angle of k_1. Directly inside this loop we increment k_1 by the ring. The location of k_1 and the angle of k_1 will determine the position of the $\vec{P}$-vector for the interaction. The ring location of k_1 will determine the λ-scaling factor for the corresponding set of $k_1 - k_3$ interactions that have the same angle orientation as k_1. This will allow us to calculate the locus coordinates and the geometric product factors for all the interactions in this set. The k_3-incrementation takes place in the two inner loops. The density function is calculated using the k_1, k_2, k_3, and k_4 values for the given interaction.

31. The basic loci contain all the possible orientations of $\vec{k}_1$ and $\vec{k}_3$, but sometimes this orientation needs to be rotated to another section of the grid. Simple rotation procedures can be used when the θ value of k_3 is larger than the θ value of k_1. Values are tabulated in Table 5 showing that loci with $\vec{P}$-vectors of equal magnitude are equivalent although their placement in space is different. This table shows how loci from interactions with $\vec{P}$-vectors of equal magnitude can be obtained by a rotation of the basic loci. Two sets of locus coordinates are shown--one set is the specific iterated coordinates for the interaction and the other set is the rotation of the basic loci coordinates. Values show that the rotation process is as valid as iterating each specific locus. Table 5 refers to rotations where θ_3 is greater than θ_1, and this rotation procedure is the same as using a rotation matrix on the basic loci coordinates (in polar coordinates this reduces to addition of a rotation angle).

Table 5

Rotated Loci

Basic Locus Coordinates (Iterated)		Iterated Locus Coordinates		Basic Locus Coordinates Rotated 3°		Iterated Locus Coordinates		Basic Locus Coordinates Rotated 6°	
k_{1x} = 0.1		k_{1x} = 0.09986		k_{1x} = 0.09986		k_{1x} = 0.09945		k_{1x} = 0.09945	
k_{1y} = 0.0		k_{1y} = 0.00523		k_{1y} = 0.00523		k_{1y} = 0.01045		k_{1y} = 0.01045	
k_{3x} = 0.10985		k_{3x} = 0.1094		k_{3x} = 0.10940		k_{3x} = 0.10865		k_{3x} = 0.10865	
k_{3y} = 0.00576		k_{3y} = 0.0115		k_{3y} = 0.01150		k_{3y} = 0.01721		k_{3y} = 0.01721	
x	y	x	y	x	y	x	y	x	y
0.1229	0.0719	0.1190	0.0782	0.1190	0.0782	0.0147	0.0843	0.0147	0.0838
0.1179	0.0788	0.1137	0.0848	0.1136	0.0848	0.1091	0.0906	0.1090	0.0906
0.1118	0.0846	0.1073	0.0904	0.1072	0.0903	0.1024	0.0958	0.1088	0.0965
0.1048	0.0893	0.1000	0.0946	0.1000	0.0946	0.0949	0.0997	0.0949	0.0997
0.0973	0.0926	0.0923	0.0976	0.0923	0.0976	0.0871	0.1023	0.0871	0.1023
0.0895	0.0948	0.0844	0.0993	0.0844	0.0993	0.0791	0.1036	0.0791	0.1036
0.0816	0.0957	0.0765	0.0999	0.0765	0.0999	0.0712	0.1037	0.0711	0.1037
0.0739	0.0957	0.0687	0.0994	0.0688	0.0994	0.0635	0.1029	0.0635	0.1029
0.0665	0.0948	0.0615	0.0981	0.0614	0.0981	0.0562	0.1012	0.0562	0.1012
0.0595	0.0931	0.0545	0.0961	0.0545	0.0961	0.0494	0.0988	0.0494	0.0988

32. Situations will exist where the θ value of $\vec{k}_1$ is larger than the θ value of k_3. An example is when k_1 has a θ value of 9° and k_3 has a value of 0°. A set of basic loci has not been defined for this condition, but there are data for an interaction that has a $\vec{P}$-vector of equal magnitude. Figure 8 shows two interactions with equal $\vec{P}$-vectors. The data for the $\vec{P}_2$-locus are given in the basic loci and the data for $\vec{P}_1$ can be calculated by a rotation of the $\vec{P}_2$ data. $\vec{P}_r$ shows the geometrical orientation of $\vec{P}_1$. Table 6 shows 10 coordinates of two loci with $\vec{P}$-vectors of the same magnitude. The third locus has been obtained by using a rotation procedure on locus 1. The rotation procedure amounts to entering the negative value of the θ_2 of locus 1 and adding θ_3 to the $-\theta_2$ for the angle coordinate of the rotated locus. Comparison of the locus coordinates of the rotated locus to locus 2 shows that they are the same locus although the corresponding increment numbers may be different.

33. The integration arrays are filled using the convention that k_3 is always larger than k_1. To include the values for the transfer for a situation where k_1 is larger than k_3, the program interchanges the k_1 and k_3 indices and enters a negative value equivalent to the original $k_1 - k_3$ transfer in the final integral array. The program ends with the evaluation of dn/dt by using a summation technique for each point of the grid.

Results

34. Figure 11 shows the contoured $\frac{dn}{dt}$ integration results for the Pierson-Moskowitz spectrum that Webb obtained using his program technique. Figure 12 shows the contoured $\frac{dn}{dt}$ results obtained using the integration technique discussed in the body of this report and the Pierson-Moskowitz spectral function. Note that the contour plot in Figure 12 plots the wave number (or radial value) on the x-axis and the θ-value on the y-axis. Contour values in Figure 12 are multiplied by 10^{-5}. Comparison of the two contours show similar behavior, and numerical results agree very closely. Note that Webb's contour plot uses

Table 6

Comparison of a Locus Obtained by Rotating a Locus with a $\hat{P}$-Vector of Equal Magnitude to the Actual Iterated Locus

Iterated Basic Locus 1 $k_1 = 0.14$ $k_3 = 0.168$ $\theta_1 = 0°$ $\theta_3 = 9°$				Iterated Locus 2 $k_1 = 0.14$ $k_3 = 0.168$ $\theta_1 = 9°$ $\theta_3 = 0°$				Rotated Locus from Iterated Locus 1 $k_1 = 0.14$ $k_3 = 0.168$ $\theta_1 = 9°$ $\theta_3 = 0°$			
Increment Number	Locus Coordinates k_2	θ_2	Geometric Product $\times 10^{-4}$	Increment Number	Locus Coordinates k'_2	θ'_2	Geometric Product $\times 10^{-4}$	Increment Number	Locus Coordinates k'_2	θ'_2	Geometric Product $\times 10^{-4}$
5	0.2704	58.18°	0.203	5	0.2703	-23.58°	0.608	5	0.2704	-49.18°	0.203
4	0.2769	55.12°	0.288	4	0.2768	-26.65°	0.652	4	0.2769	-46.12°	0.288
3	0.2819	51.94°	0.386	3	0.2819	-29.83°	0.664	3	0.2819	-42.90°	0.386
2	0.2842	48.68°	0.488	2	0.2850	-33.08°	0.639	2	0.2842	-39.68°	0.488
1	0.2859	45.38°	0.577	1	0.2860	-36.38°	0.577	1	0.2859	-36.38°	0.577
50	0.2850	42.08°	0.639	50	0.2849	-39.68°	0.488	50	0.2850	-33.08°	0.639
49	0.2818	38.83°	0.664	49	0.2819	-42.94°	0.386	49	0.2818	-29.83°	0.664
48	0.2768	35.65°	0.652	48	0.2768	-46.12°	0.288	48	0.2768	-26.65°	0.652
47	0.2703	32.58°	0.608	47	0.2704	-49.18°	0.203	47	0.2703	-23.58°	0.608
46	0.2625	29.65°	0.544	46	0.2624	-52.13°	0.137	46	0.2625	-20.65°	0.544
45	0.2536	26.86°	0.470	45	0.2537	-54.91°	0.088	45	0.2536	-17.86°	0.470

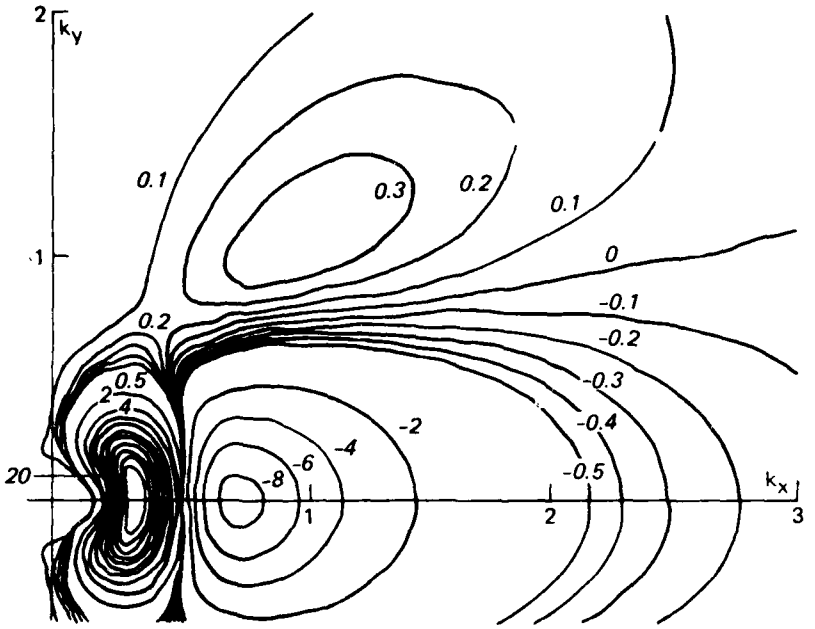

Figure 11. The nonlinear transfer dn/dt as a function of wave number. The contours are marked in units of 10^{-3} MKS units (from Webb 1978)

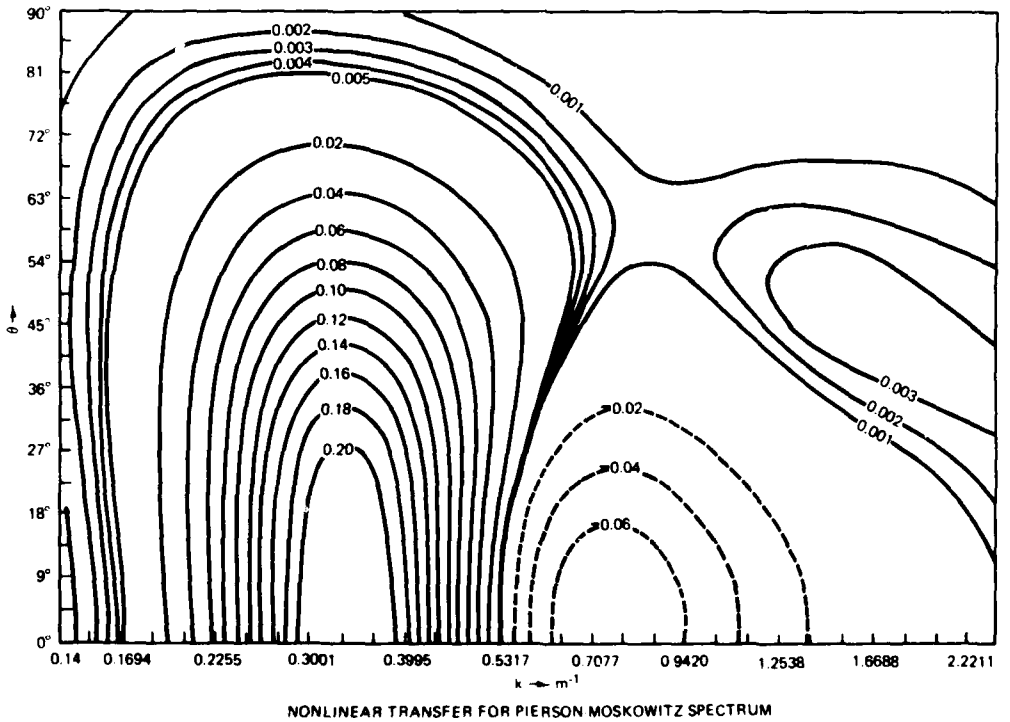

Figure 12. Contour plot of the nonlinear energy transfer for the Pierson-Moskowitz spectrum (all contour values are multiplied by 10^{-5}) as a function of wave-number magnitude and direction (Tracy 1979)

Cartesian coordinates for the wave numbers. The computer time for the Pierson-Moskowitz spectrum using 30 values of k ($0.14\ m^{-1}$ to $2.44\ m^{-1}$) and angular increments from -90° to +90° in 4.5° increments was 151 sec on the CRAY computer.

35. The Pierson-Moskowitz spectrum was used initially so results from our technique could be compared with Webb's results using the same spectrum. The JONSWAP researchers list a general analytical form for a spectral density function (Sell and Hasselmann 1972). It contains various shape parameters, γ, σ_a, and σ_b, that can be varied easily in the computer coding. This spectral density function can be written as:

$$E(f) = \alpha g^2 (2\pi)^{-4} f^{-5} \exp\left[\frac{-5}{4}\left(\frac{f}{f_m}\right)^{-4}\right] \gamma^{\exp \frac{-(f - f_m)^2}{2\sigma^2 f_m^2}} \qquad (43)$$

where

$$f_m = 0.3$$

$$\alpha = 0.01$$

$$\sigma = \begin{cases} \sigma_a \text{ for } f \leq f_m \\ \sigma_b \text{ for } f > f_m \end{cases}$$

where α is the equilibrium range coefficient, f_m is the frequency of the spectral peak, γ is the peak enhancement parameter and σ_a and σ_b are the left and right spectral widths of the spectrum. f_m and α were treated as constants for the various spectra. This density function was used with a $\cos^2 \theta$ spreading function. The Pierson-Moskowitz spectrum corresponds to $\gamma = 1$, $\sigma_a = 0.07$, and $\sigma_b = 0.09$. Various combinations of shape parameters were run and computer times are similar to the run time for the Pierson-Moskowitz spectrum.

36. Figures 13-17 give the results of the calculations of the net source functions for various spectra of the type described by Equation 43. These results are given in terms of angularly integrated functions since these are easier to visualize than the corresponding two-dimensional source functions. Figure 13 shows the one-dimensional energy transfer function for the Pierson-Moskowitz spectrum ($\gamma = 1$, $\sigma_a = 0.07$,

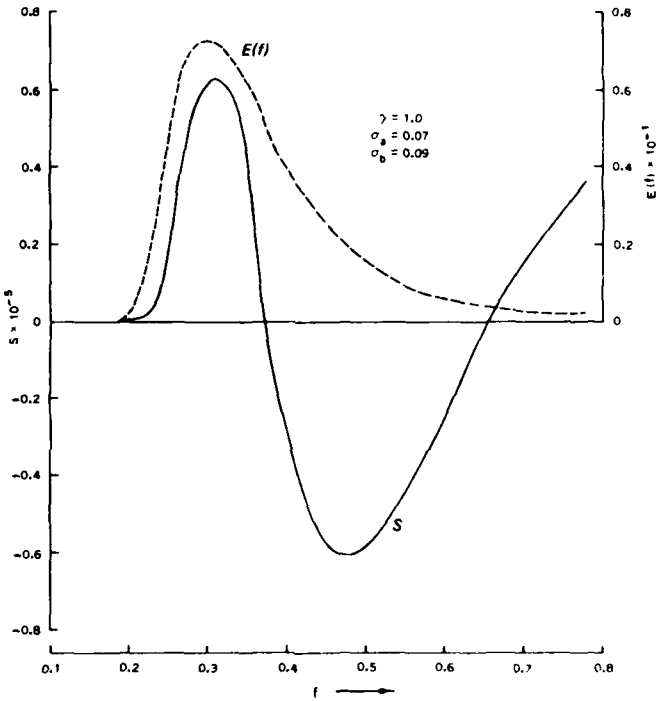

Figure 13. The one-dimensional nonlinear energy transfer (S) and the energy [E(f)] as a function of frequency for the Pierson-Moskowitz spectrum

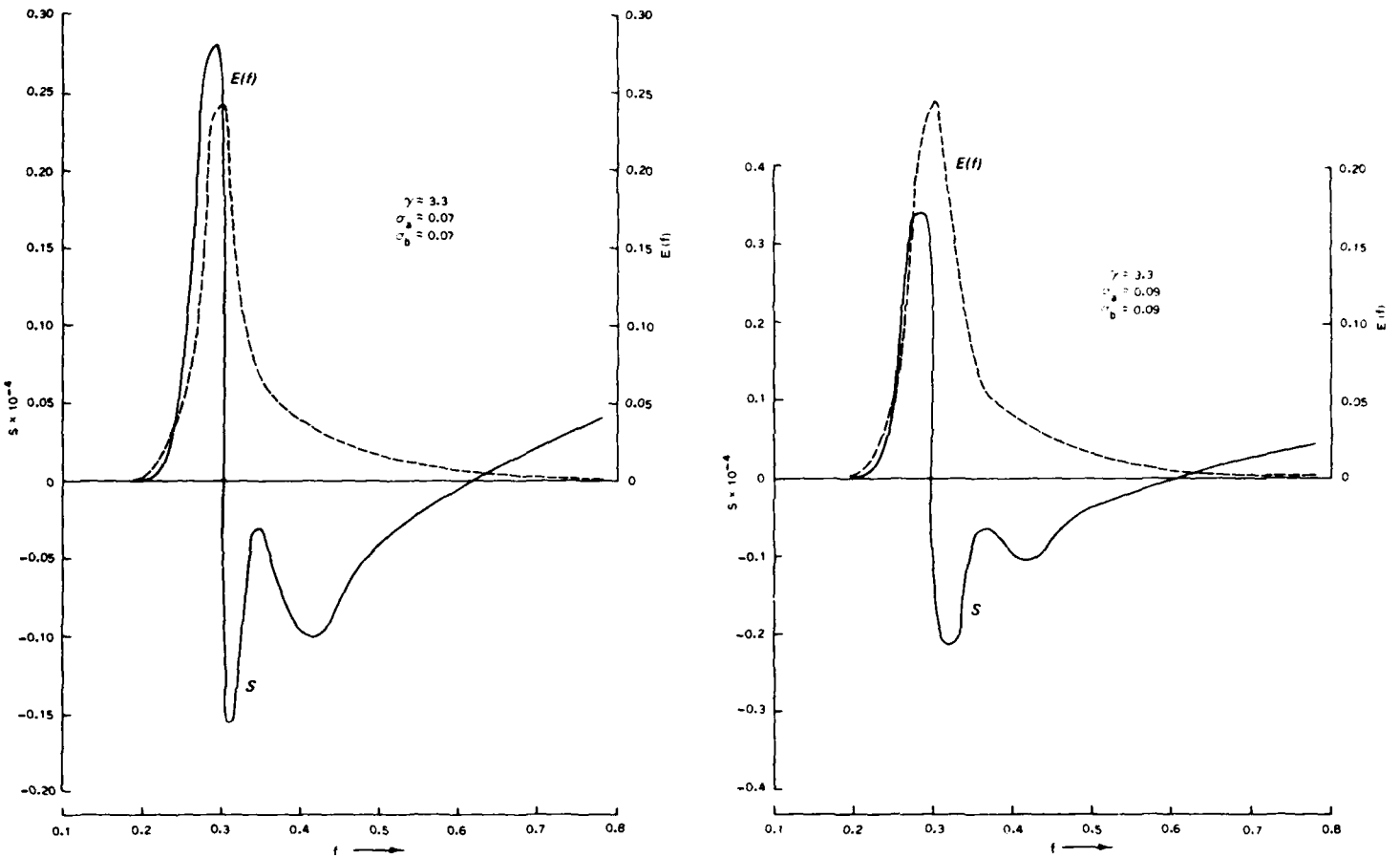

Figure 14. The nonlinear energy transfer (S) and the input energy [E(F)] as a function of frequency for four JONSWAP frequency spectra with $\gamma = 3.3$ and different shape parameters (Continued)

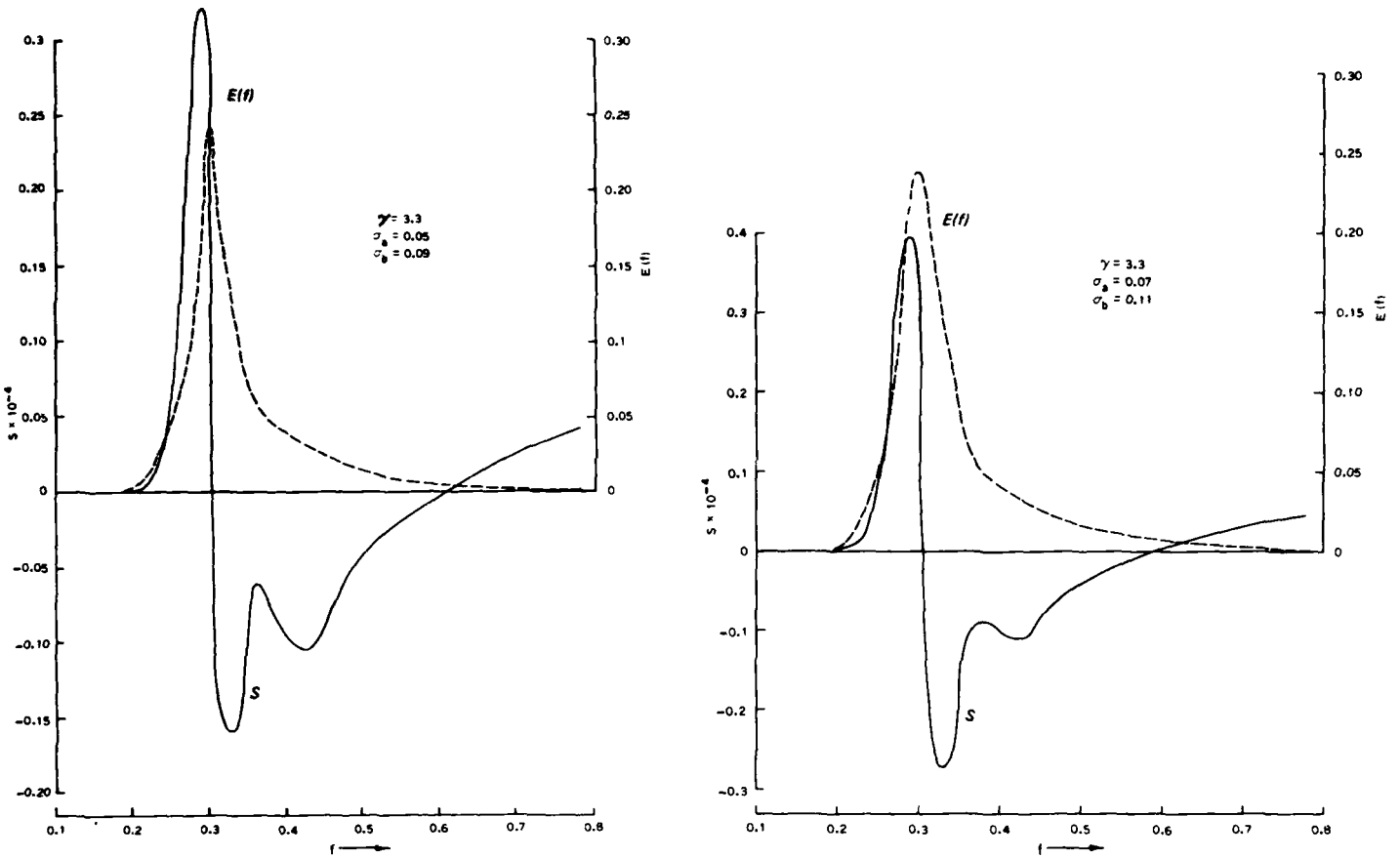

Figure 14. (Concluded)

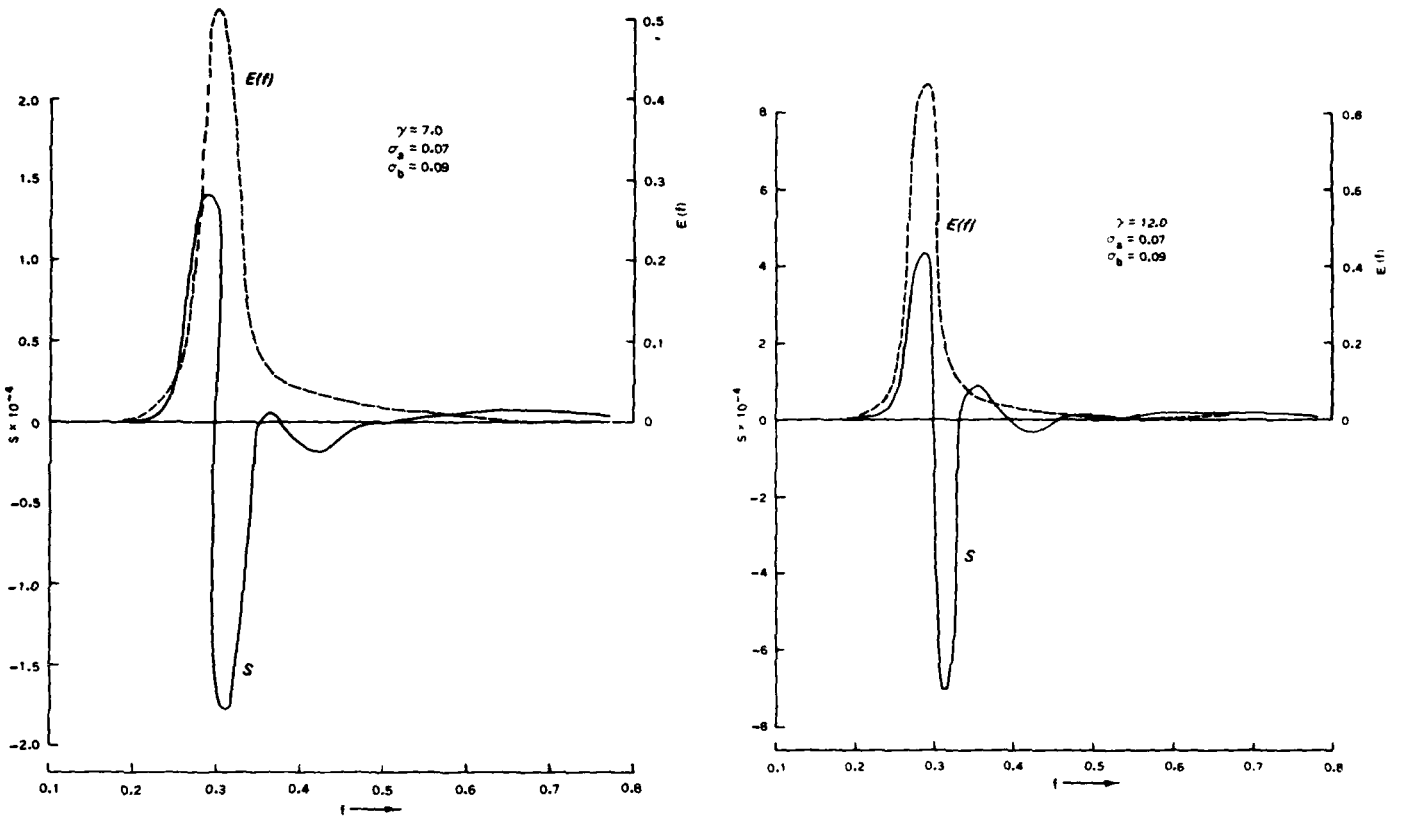

Figure 15. The nonlinear energy transfer (S) and the input energy [E(f)] as a function of frequency for two sharp JONSWAP frequency spectra

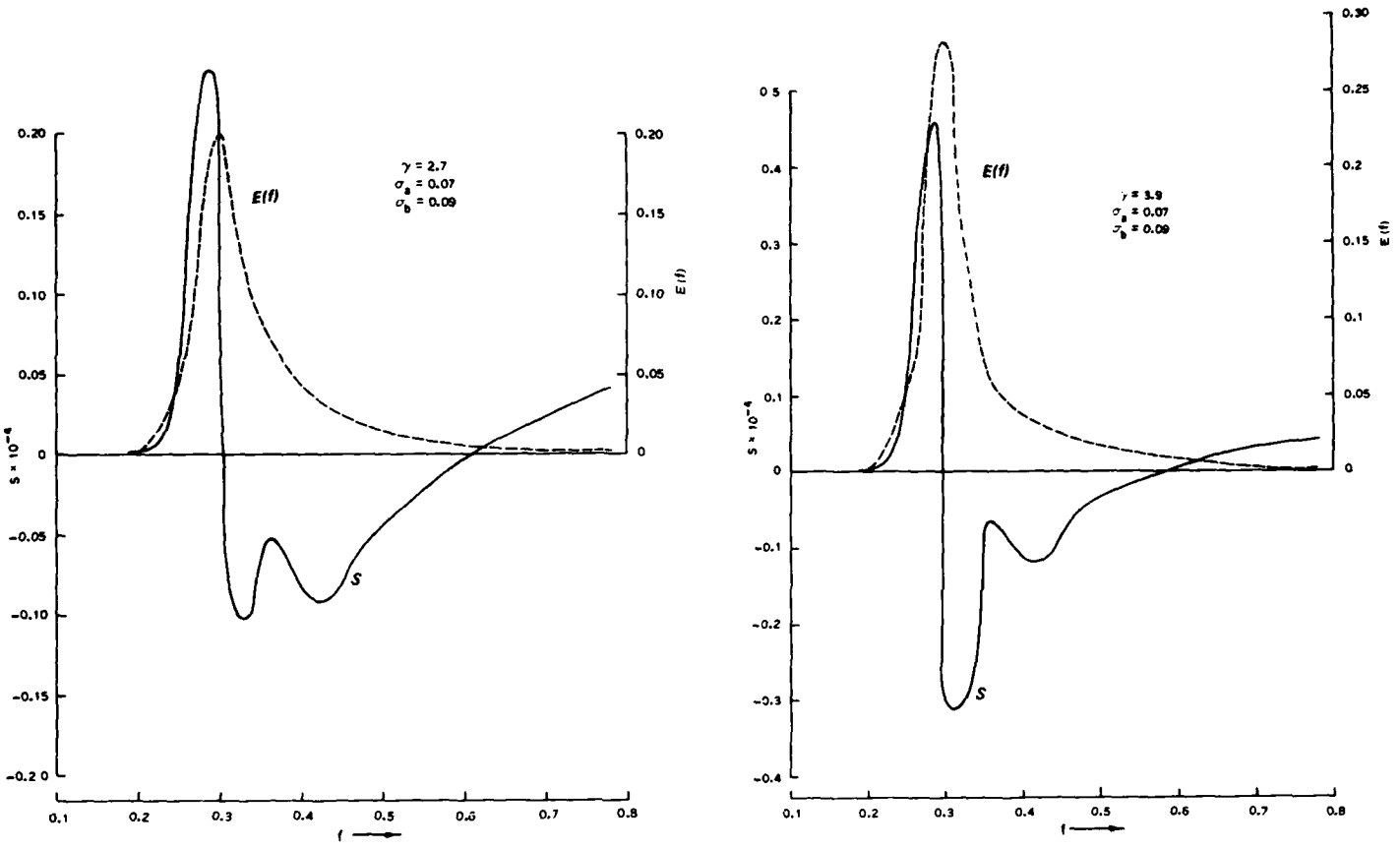

Figure 16. The nonlinear energy transfer (S) and the input energy [E(f)] as a function of frequency for three JONSWAP frequency spectra (Continued)

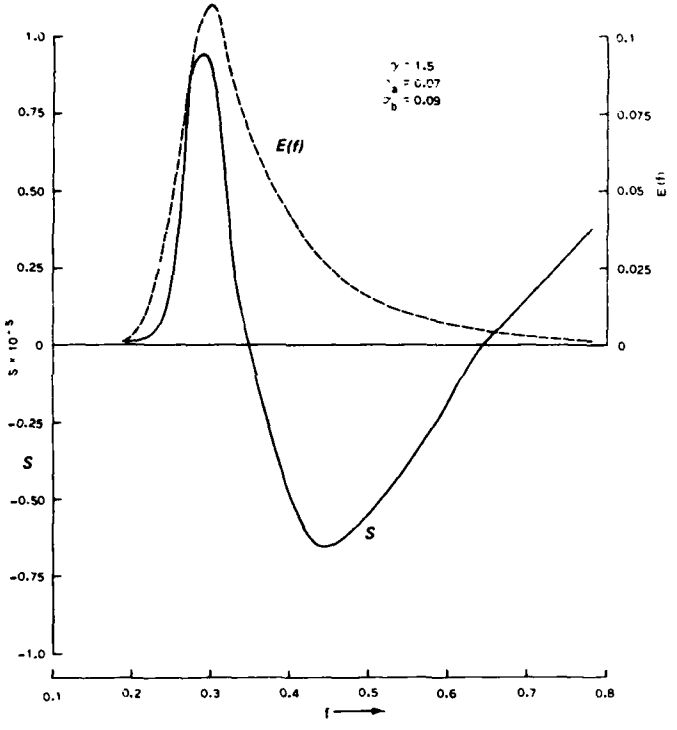

Figure 16. (Concluded)

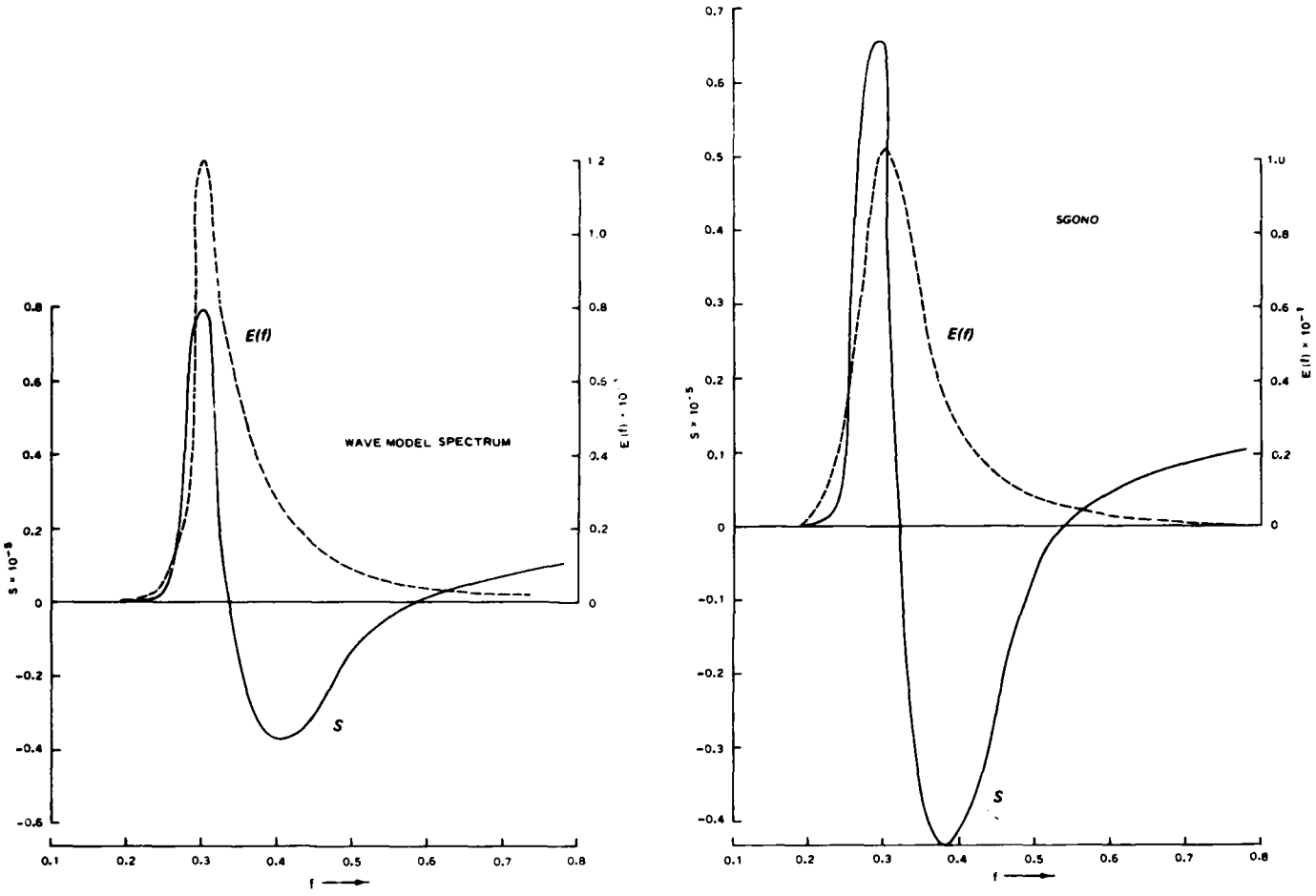

Figure 17. The nonlinear energy transfer (S) and the input energy E(f) as a function of frequency for the Wave Model Spectrum and the SGONO spectrum

$\sigma_b = 0.09$) . The one-dimensional transfer rate is calculated by $S(f) = \int S(f,\theta)\, d\theta$ where $S(f,\theta)$ is $\frac{\partial n}{\partial t}$ and is graphed in Figure 13 and Figures 14-17 as a function of frequency. The spectral energy is graphed on the right-hand side of the graph and is also a function of frequency. Figure 13 can be compared with the JONSWAP results for the Pierson-Moskowitz spectrum (Sell and Hasselmann 1972). Figures 14-16 can also be compared with the JONSWAP results (Sell and Hasselmann 1972). Two spectra that do not correspond to the JONSWAP analytical expression were treated in Figure 17. The wave model spectrum has an f^{-5} tail and the forward face of the spectrum is represented by $\left\{\exp\left[-(f_m/f)^2\right] E_{f_m}\right\}$ where $f_m = 0.3$ and $E_{f_m} \alpha f_m^{-5}$. The SGONO spectrum also contains the f^{-5} tail and $f_m = 0.3$. The slope of the forward face of the spectrum was determined from the input wind speed to create an $f_m = 0.3$. E is in M^2/Hz and S or $\frac{\partial n}{\partial t}$ is calculated in MKS units. Results indicate that this approach to calculation of the nonlinear energy transfer agrees with previous research and is an efficient process.

37. In a comparison of the S-curves in Figures 13 and 14-17 a similar behavior is observed. This behavior shows the source-sink effect of the nonlinear interactions within the spectrum. The variation of the peak enhancement factor, γ , shows that as the spectrum becomes steeper the negative lobe of the wave-wave interactions shows a trend toward the positive and in the very steep spectra the function even develops a slight positive lobe within the usual negative region. In the steepest spectra the nonlinear curve, S , approaches a sinusoidal damping curve. The steep spectrum acts like a single energy packet at a certain Δf range and shows how the nonlinear reactions attempt to create a more stable spectral form.

Discussion

38. The main result of this report is to provide an efficient integration technique to evaluate Boltzmann integrals of the type derived for energy transfer due to wave-wave interaction in a wave spectrum.

In the past, evaluation of these integrals required extensive computer time. Webb's transformation of the form of the integrals simplified the mathematics but did not significantly reduce the computational time for their calculation. This report has demonstrated that by a straight forward transformation of the integration space, a large increase in computational efficiency is achieved. Webb has discussed various physical aspects of the results of the nonlinear transfer and the JONSWAP study has shown these results in their experimental data. The reader is referred to these papers for a complete discussion of these results.

39. Specialized numerical techniques and grids set up for a specific problem are often only useful in one specific problem and have no relation to the physical problem. The technique developed in this paper sets up a series of similar triangles for a given θ_3 and θ_1 orientation as shown in Figure 7. This sets up a similarity relation between the energy transfer of the various $\vec{P}$-vectors shown at a given $\theta_3 - \theta_1$ orientation. If a situation exists where the density function scales, the nonlinear transfer at a fixed-angle difference could be evaluated by a summation. The approach outlined in this report follows the actual physics of the interactions and gives a geometrical insight into the actual process without obscuring the process with complex mathematical manipulation. These concepts will be useful in describing the complex nature of nonlinear wave-wave interactions.

References

Forristall, G. Z. et al. 1978. "The Directional Spectra and Kinematics of Surface Gravity Waves in Tropical Storm Delia," Journal of Physical Oceanography, Vol 8, pp 888-909.

Hasselmann, K. 1962. "On the Non-Linear Energy Transfer in Gravity-Wave Spectrum; 1: General Theory," Journal of Fluid Mechanics, Vol 12, pp 481-500.

Jackson, J. D. 1962. Classical Electrodynamics, Wiley, New York.

Sell, W., and Hasselmann, K. 1972. "Computations of Non-Linear Energy Transfer for JONSWAP and Empirical Wind Wave Spectra," Institute of Geophysics, University of Hamburg, Hamburg, Germany.

Tracy, F. T. 1979. "A Computer Program for Contouring the Output of Finite Element Programs," U. S. Army Engineer Waterways Experiment Station, CE, Vicksburg, Miss.

Webb, D. J. 1978. "Non-Linear Transfers Between Sea Waves," Deep-Sea Research, Vol 25, pp 279-298.

Bibliography

Hasselmann, K. et al. 1973. "Measurements of Wind-Wave Growth and Swell Decay During the Joint North Sea Wave Project," *Deutsches Hydrographisches Institut*, Hamburg, Germany.

Tracy, B. A. 1981. Calculation of the Non-Linear Energy Transfer Between Sea Waves Using a Geometrically-Spaced Grid, M.S. Thesis, Department of Mechanical Engineering, Mississippi State University, Mississippi State, Miss.

Appendix A: Computing Notes

This is the subroutine used to calculate the coupling coefficient. The equation for the coupling coefficient is given by Webb (1978). In the subroutine below WK1 corresponds to K_1, X_1 corresponds to K_{X1} etc.

```
      FUNCTION CPLE(X1,Y1,X2,Y2,X3,Y3,X4,Y4,IPP)
      IPP=0
      WK1=SQRT(X1*X1+Y1*Y1)
      WK2=SQRT(X2*X2+Y2*Y2)
      WK3=SQRT(X3*X3+Y3*Y3)
      WK4=SQRT(X4*X4+Y4*Y4)
      W1=SQRT(WK1)
      W2=SQRT(WK2)
      W3=SQRT(WK3)
      W4=SQRT(WK4)
      DOT12=X1*X2+Y1*Y2
      DOT13=X1*X3+Y1*Y3
      DOT14=X1*X4+Y1*Y4
      DOT23=X2*X3+Y2*Y3
      DOT24=X2*X4+Y2*Y4
      DOT34=X3*X4+Y3*Y4
      WSQP12=SQRT((X1+X2)*(X1+X2)+(Y1+Y2)*(Y1+Y2))
      WSQ12=(W1+W2)*(W1+W2)
      Z=2.*WSQ12*(WK1*WK2-DOT12)*(WK3*WK4-DOT34)
      P1=Z/(WSQP12-WSQ12)
      WSQM13=SQRT((X1-X3)*(X1-X3)+(Y1-Y3)*(Y1-Y3))
      WSQ13=(W1-W3)*(W1-W3)
      Z=2.*WSQ13*(WK1*WK3+DOT13)*(WK2*WK4+DOT24)
      P2=Z/(WSQM13-WSQ13)
      WSQM14=SQRT((X1-X4)*(X1-X4)+(Y1-Y4)*(Y1-Y4))
      WSQ14=(W1-W4)*(W1-W4)
      Z=2.*WSQ14*(WK1*WK4+DOT14)*(WK2*WK3+DOT23)
      P3=Z/(WSQM14-WSQ14)
      P4=0.5*(DOT12*DOT34+DOT13*DOT24+DOT14*DOT23)
      P5=.25*((DOT13+DOT24)*WSQ13*WSQ14-(DOT12+DOT34)
     *WSQ12*WSQ12)
      P6=0.25*(DOT14+DOT23)*WSQ14*WSQ14+2.5*WK1*WK2*WK3*WK4
      P7=WSQ12*WSQ13*WSQ14*(WK1+WK2+WK3+WK4)
      IF (IPP.EQ.1) PRINT 100,P1,P2,P3,P4,P5,P6,P7
  100 FORMAT (1X,7F10.4)
      D=P1+P2+P3+P4+P5+P6+P7
      D=D*D
      CPLE=0.785398*D/(W1*W2*W3*W4)
      RETURN
      END
```

Appendix B: Notation

a	Dummy variable for delta function
c_g	Group velocity
$C(\vec{k}_1, \ldots)$	Coupling coefficient
$D(\vec{k}_1, \ldots)$	Density function
E	Energy
f	Frequency
f_m	Frequency of peak of spectrum
$F(\vec{k}_1, \ldots)$	Product of coupling coefficient, $\theta(x)$, and density function
g	Acceleration due to gravity
$GEOM(\vec{k}_1, \ldots)$	Geometric product
$\vec{k}_1$	Wave-number vector for i^{th} wave number
k_1	$\lvert\vec{k}_1\rvert$
k_o	Smallest value of r on (r,θ) grid
n_i	Action density of i^{th} wave number
$\vec{n}$	Normal (radial) direction in $\vec{k}_2$-space
n	Number of radial
$\vec{P}$	Interaction vector $(\vec{k}_1 - \vec{k}_3)$
Q	$k_1^{1/2} - k_3^{1/2}$ (a magnitude)
r	$\lvert\vec{k}\rvert$
$\vec{s}$	Tangential direction in k_2-space
$T(\vec{k}_1,\vec{k}_3)$	Transfer function
$W(\vec{k}_2)$	Locus equation = $Q + k_2^{1/2} - \left(\lvert\vec{P} + \vec{k}_2\rvert\right)^{1/2} = 0$
α	Phillips equilibrium constant

σ A measure of spectral width in spectral equation

γ Peak enhancement parameter in spectral equation

ω_i Angular velocity of i^{th} wave number

$\delta(...)$ Dirac delta function

λ Scaling factor in integral; geometric spacing multiple

$\theta(x)$ $\theta\left(|\vec{k}_1 - \vec{k}_4| - |\vec{k}_1 - \vec{k}_3|\right)$; has a value of 1 or 0 for integral

θ Angle measurement in polar grid

In accordance with letter from DAEN-RDC, DAEN-ASI dated 22 July 1977, Subject: Facsimile Catalog Cards for Laboratory Technical Publications, a facsimile catalog card in Library of Congress MARC format is reproduced below.

Tracy, Barbara A.
Theory and calculation of the nonlinear energy transfer between sea waves in deep water / by Barbara A. Tracy, Donald T. Resio (Hydraulics Laboratory, U.S. Army Engineer Waterways Experiment Station). -- Vicksburg, Miss. : The Station ; Springfield, Va. : available from NTIS, 1982.
47, [3] p. : ill. ; 27 cm. -- (WIS report ; 11)
Cover title.
"May 1982."
"Prepared for Office, Chief of Engineers, U.S. Army."
"Wave Information Studies of U.S. Coastlines."
Bibliography: p. 47.

1. Energy transfer. 2. Integral equations, Nonlinear. 3. Ocean waves. 4. Transport theory. 5. Water waves. I. Resio, Donald T. II. United States. Army. Corps of Engineers. Office of the Chief of Engineers. III. Wave Information Studies of U.S. Coastlines.

Tracy, Barbara A.
Theory and calculation of the nonlinear energy : ... 1982.
(Card 2)

IV. U.S. Army Engineer Waterways Experiment Station. Hydraulics Laboratory. V. Title VI. Series: WIS report (U.S. Army Engineer Waterways Experiment Station) ; 11.
TA7.W349 no.11